Journal of Nuclear Cardiology (2024) 40, 102011

STATE OF THE ART REVIEW

PET myocardial perfusion imaging: Trends, challenges, and opportunities

Jorge Dahdal, MD [1,2], Ruurt A. Jukema, MD [1], Hendrik J. Harms, PhD [3], Maarten J. Cramer, MD, PhD [4], Pieter G. Raijmakers, MD, PhD [5], Paul Knaapen, MD, PhD [1], Ibrahim Danad, MD, PhD [1,6,*]

[1] Departments of Cardiology, Amsterdam Cardiovascular Sciences, Amsterdam UMC, Vrije Universiteit Amsterdam, Amsterdam, the Netherlands
[2] Department of Cardiology, Hospital Del Salvador, Santiago, Chile
[3] MedTrace Pharma A/S, Horsholm, Denmark
[4] Department of Cardiology, University Medical Center Utrecht, Utrecht, the Netherlands
[5] Radiology, Nuclear Medicine & PET Research, Amsterdam UMC, Vrije Universiteit Amsterdam, Amsterdam, the Netherlands
[6] Department of Cardiology, Radboud University Medical Center, Nijmegen, the Netherlands

[*] Corresponding author. Department of Cardiology, Radboud University Medical Center, Geert Grooteplein Zuid 10, 6525 GA Nijmegen, the Netherlands.
E-mail address: Ibrahim.danad@radboudumc.nl (Ibrahim Danad).

Abstract

Various non-invasive images are used in clinical practice for the diagnosis and prognostication of chronic coronary syndromes. Notably, quantitative myocardial perfusion imaging (MPI) through positron emission tomography (PET) has seen significant technical advancements and a substantial increase in its use over the past two decades. This progress has generated an unprecedented wealth of clinical information, which, when properly applied, can diagnose and fine-tune the management of patients with different types of ischemic syndromes. This state-of-art review focuses on quantitative PET MPI, its integration into clinical practice, and how it holds up at the eyes of modern cardiac imaging and revascularization clinical trials, along with future perspectives.

Keywords: Positron emission tomography, Myocardial perfusion imaging, Coronary artery disease, Myocardial blood flow, Myocardial flow reserve

INTRODUCTION

The identification of myocardial ischemia has been the traditional approach for identifying high-risk chronic chest pain patients eligible for coronary revascularization therapy. However, the concept of `ischemia´ guided coronary revascularization has been challenged by randomized trials usually showing revascularization therapy failing to alter long-term outcomes when compared to optimal medical therapy. This is not surprising on itself since coronary artery disease (CAD) usually exists diffusely, and therefore, localized mechanical interventions in a narrowed segment may fail to alter the natural disease process of ongoing arterial inflammation, plaque progression and subsequent instability in the remaining segments of the coronary tree. As such, some have legitimately questioned the current role of functional non-invasive imaging in the management of chronic chest pain patients shifting towards a more anatomical based approach using coronary computed tomography angiography (CCTA). Large studies such as the Scottish Computed Tomography of the Heart

Received 11 March 2024; Accepted 19 July 2024; Available online 25 July 2024

https://doi.org/10.1016/j.nuclcard.2024.102011

ABBREVIATIONS

CAC	Coronary Artery Calcium
CAD	Coronary Artery Disease
CCTA	Coronary Computed Tomography Angiography
CFC	Coronary Flow Capacity
CMVD	Coronary Microvascular Disease
ECG	Electrocardiogram
FFR	Fractional Flow Reserve
[^{18}F] Flurpiridaz	^{18}F-Flurpiridaz
ICA	Invasive Coronary Angiography
MBF	Myocardial Blood Flow
MFR	Myocardial Flow Reserve
MI	Myocardial Infarction
MPI	Myocardial Perfusion Imaging
[^{13}N]NH_3	^{13}N-ammonia
[^{15}O]H_2O	^{15}O-Water
PET	Positron Emission Tomography
RFR	Relative Flow Reserve
^{82}Rb	^{82}Rubidium
SPECT	Single-Photon Emission Computed Tomography

(SCOT-HEART) and Prospective Multicenter Imaging Study for Evaluation of Chest Pain (PROMISE) trial have further challenged the idea of perfusion imaging guided management [1,2]. The SCOT-HEART trial underscored CCTA's added value on clinical decision-making by presumably improving patient compliance and hence clinical outcomes. This reduced the composite outcome of cardiovascular death and myocardial infarction (MI) in comparison to the standard care arm (2.3% vs 3.9%; hazard ratio (HR) = .59, 95% CI: .41-.84; $P = .004$) [1]. Moreover, the Clinical Outcomes Utilizing Revascularization and Aggressive Drug Evaluation (COURAGE) nuclear sub-study and the International Study of Comparative Health Effectiveness with Medical and Invasive Approaches (ISCHEMIA) trial indicated that revascularization stratified by ischemia assessment did not prevent coronary events more effectively than medical treatment [3,4]. Both trials also demonstrated that the anatomical severity and extent of CAD are the most important predictors of MI and mortality. Several hypotheses have been postulated on the failure of myocardial perfusion imaging (MPI) in directing revascularization therapy to prevent future coronary events in chronic coronary syndrome patients. A prevalent perspective is that the dominant stress testing techniques used in the referred studies are relatively outdated and deficient in precisely detecting subendocardial ischemia, let alone an adequate delineation of its extent and depth. Second, a flaw in current practice when interpreting MPI is to consider ischemia a binary phenomenon and therefore not exploiting the potential of contemporary quantitative MPI that allows for delineation of the complete spectrum of ischemic heart disease [5,6].

In recent years, the utilization of positron emission tomography (PET) MPI has seen a steady rise. This is evident in the United States where the use of PET in cardiology offices nearly tripled between 2010 and 2019 [7]. This trend is expected to continue, with PET outpatient services projected to grow more than 60% over the next 5 years [8]. The rise in PET use can be attributed to its superior diagnostic performance in detecting ischemia, enhanced image quality, one-day protocols, and lower radiation doses compared to single-photon emission computed tomography (SPECT) and especially its potential to accurately quantify myocardial blood flow in absolute terms [9–11]. In this review, we will delve into the modern applications of quantitative cardiac PET for ischemic heart disease. We will further elaborate on the fundamental factors that sustain the strength of this diagnostic technique in an era in which the role of functional imaging is questioned following ISCHEMIA trial and the increasing clinical importance of CCTA.

PET MPI RADIOTRACER CHARACTERISTICS

The evolution of PET MPI reflects a series of ground-breaking advancements in medical imaging. A timeline overview of key milestones in the development of PET MPI is displayed in Figure 1 [12–14]. A detailed discussion of PET physics and technical aspects is beyond the scope of this article; these topics are covered elsewhere. [15–18].

Several tracers are utilized for PET MPI, each with distinct characteristics as outlined in Table 1. Among these tracers, ^{82}Rubidium (^{82}Rb) and ^{13}N-ammonia ([^{13}N]NH_3) have been predominantly employed in clinical settings, having received approval from regulatory bodies over 15 years ago. In contrast, ^{15}O-water ([^{15}O]H_2O) and ^{18}F-Flurpiridaz ([^{18}F]Flurpiridaz) have primarily been explored within research contexts, and are currently investigated for broader clinical applications [19,20]. Notably, there exists extensive clinical expertise with [^{15}O]H_2O in some European and Asian academic centers. Attractively, the rapid decay of ^{82}Rb and [^{15}O]H_2O enables fast stress and rest imaging protocols (less than 30 minutes). In addition, radiation dose to the patient is lower than for [^{13}N]NH_3 or [^{18}F]Flurpiridaz, simply due to

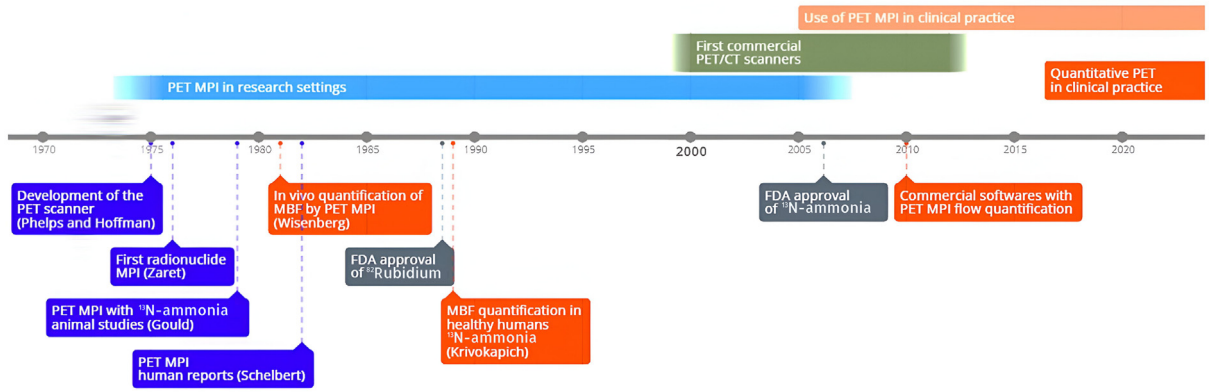

Figure 1. Milestones in PET MPI development. Since the inception of radionuclide MPI in 1973, the field of nuclear medicine has witnessed an impressive trajectory of progress, characterized by advancements in radiopharmaceuticals tracers and imaging technology. The first animal study using PET to assess myocardial perfusion was conducted by Gould et al. at the University of California's division of Nuclear Medicine [12]. Using ^{13}N-ammonia as a tracer, they correlated experimentally induced stenosis in dogs with stress-induced myocardial perfusion abnormalities. This laid the foundation for the first human research 3 years after, in which PET MPI accurately identified the majority of stenoses in a study population entailing healthy participants and patients with known CAD [13]. Later, others studies demonstrated the accuracy of cardiac PET as a non-invasive method for quantifying myocardial blood flow, using radioactively labelled albumin microspheres as the gold standard for quantitative myocardial perfusion [14]. In this early stage, PET was primarily considered a research tool due to its technical complexity, cost, and limited availability. However, a shift occurred in the early 2000s when the firsts commercial clinical PET-CT systems were introduced. This opened the door for cardiac PET-CT to transition from research labs to the clinical setting, significantly expanding its use concerning the management of CAD. This transition has been followed by concurrent advancements in hardware development, radiotracer availability, and image post-processing software. Moreover, over the past decade, the introduction of software packages that can derive quantitative MBF data from dynamic scans has further broadened the clinical applications of this method.

the duration of exposure being shorter than for these longer-lived radioisotopes (Table 1). The short half-life tracers need to be produced on-site. For instance, ^{82}Rb can be generated using commercially available generators that provide ^{82}Rb on-site. Due to its short half-life of approximately 76 seconds, ^{82}Rb is favored for its ease of on-site production by generators and rapid imaging protocols. The availability of commercial ^{82}Rb generators enhances the practicality of PET MPI, allowing for timely and efficient imaging protocols. However, the generators have a limited operational lifespan, typically needing replacement every 4-6 weeks. Therefore, an efficient and streamlined protocol is necessary to maximize cost efficiency and ensure the generator's capacity is fully utilized before it is depleted. On the other hand, producing [^{13}N]NH_3 and [^{15}O]H_2O requires an on-site cyclotron necessitating a dedicated production infrastructure, which can be cost-prohibitive for most clinical PET centers. Due to its long half-life [^{18}F]Flurpiridaz tracers can be produced at a central facility (off-site) and distributed to hospitals across a broader region, similar to for example fluorodeoxyglucose PET. The choice for a specific tracer in PET MPI is influenced by various factors including the availability of production facilities, the desired diagnostic accuracy and clinical use, and the workflow considerations.

When assessing the capacity for flow quantification, it is essential to understand that tracers such as [^{15}O]H_2O, [^{13}N]NH_3, and [^{18}F]Flurpiridaz exhibit an uptake rates (K_1) that increases proportionally to myocardial blood flow (MBF), whereas ^{82}Rb uptake reaches a plateau at high flow rates (Figure 2). Another downside of ^{82}Rb is its relatively lower image resolution compared to other PET tracers, primarily due to its higher positron range (2.60 mm) [22]. Additionally, as blood flow rise, the myocardial extraction of ^{82}Rb levels off (Figure 2A), resulting in a non-linear relationship between tracer uptake and MBF at high flow rates (Figure 2B) [23]. This phenomenon, termed the `roll-off phenomenon,´ results in suboptimal signal-to-noise ratio [24,25]. Consequently, corrections are necessary to address the limited extraction, but these adjustments invariably amplify noise. Consequently, even a small error in the ^{82}Rb uptake rate (K_1) value can significantly skew estimates of MBF, whereas similar errors have less impact on calculated MBF values for other PET perfusion tracers (Figure 2B). Remarkably, [^{15}O]H_2O stands out as the only tracer where the washout rate (K_2) is used for MBF quantification [26]. Similar to K_1, K_2 is directly

Table 1. Characteristics of tracers used for PET MPI imaging.

Characteristic	$[^{15}O]H_2O$	$[^{13}N]NH_3$	^{82}Rb	$[^{18}F]$Flurpiridaz
Tracer production	On-site cyclotron	On-site cyclotron	Generator	Off-site cyclotron
Tracer half-life	123 seconds	9.96 minutes	76 seconds	110 minutes
Positron range	1.02 mm	.57 mm	2.60 mm	.23 mm
First pass extraction fraction	~ 100%	~ 80%	~ 65%	>90%
Kinetics	Freely diffusible, metabolically inert	Metabolically trapped in myocardium	Metabolically trapped in myocardium	Metabolically trapped in myocardium
Flow quantification	Excellent	Good	Moderate	Very good
Effective radiation dose	~ .4 mSv/370 MBq	~ 1 mSv/550 MBq	~ .7 mSv/555 MBq	~ 2.1 mSv/111 MBq (rest) ~ 6.6 mSv/351 MBq (exercise) ~ 4.6 mSv/244 MBq (pharmacological stress)
Image quality	Good (parametric MBF images)	Very good	Good	Excellent
Gating/LV function	−/+	+	+	+
Exercise protocol compatible	−	−	−	+

proportional to MBF [27]. However, while K_1 is significantly influenced by partial volume effects, K_2 is less affected by these artifacts, making it more reliable for converting to MBF. Scar tissue or areas with limited perfusion affect the amplitude of the time activity curve but not its shape. Likewise, attenuation artifacts are less likely to alter the shape of the washout rate. Hence, MBF can be accurately measured using $[^{15}O]H_2O$ without requiring corrections for attenuation, eliminating the need for a low-dose CT scan [27–29]. Nevertheless, calculating the perfusable tissue index, a surrogate for scar tissue, necessitates the anatomical tissue fraction obtained from a low-dose CT scan. While $[^{15}O]H_2O$ is metabolically inert and freely diffusible rendering it an ideal tracer for flow quantification, other flow tracers are retained in the myocardium providing qualitative perfusion images (relative distribution images) with high diagnostic quality and facilitate ECG-gated assessments for left ventricle (LV) ejection fraction [30–32]. Although this was initially challenging with $[^{15}O]H_2O$, recent advances have shown that it is feasible using cardiac-gated parametric blood volume images with these measurments showing a strong correlation with LV volumes derived from cardiac magnetic resonance (CMR) [33,34]. In addition, myocardial viability can be traditionally assessed with relative perfusion images. For $[^{15}O]H_2O$ PET MPI, resting MBF, the perfusable tissue fraction and the perfusable tissue index have been

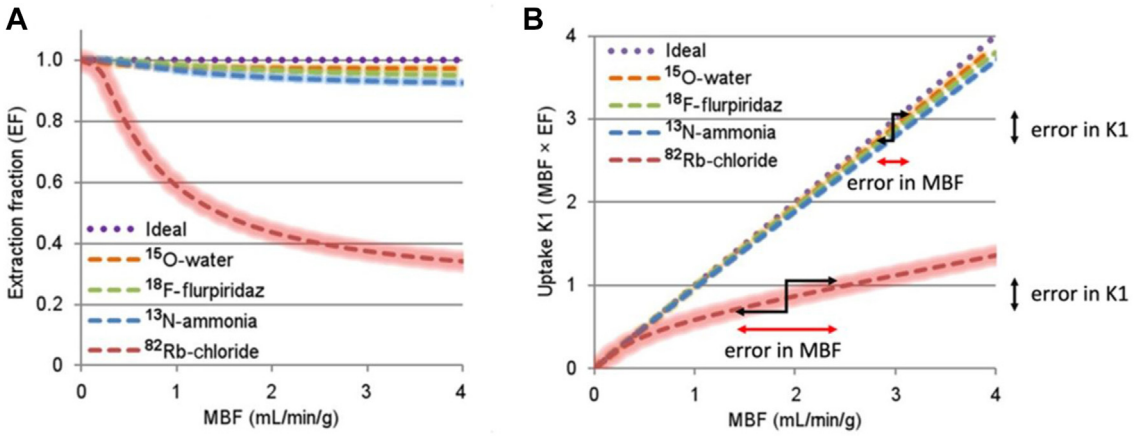

Figure 2. Radiotracer extraction fractions (A) and uptake rates (B) with a compartmental model. Influence of K_1 errors on calculated myocardial blood flow values for $[^{15}O]H_2O$ and ^{82}Rb tracer. Adapted from Murthy et al. [21].

evaluated as markers of myocardial viability [35–38]. In a recently published study by Hoff et al. [^{15}O]H_2O was demonstrated to be non-inferior to ^{82}Rb for detection of scar tissue [39].

DIAGNOSTIC PERFORMANCE OF PET MPI FOR THE DETECTION OF CORONARY ARTERY DISEASE

There is a wealth of data supporting the diagnostic application of PET MPI for the detection of CAD. Table 2 provides a synopsis of the outcomes derived from various meta-analyses comparing the diagnostic yield of stress imaging in patients with chronic coronary syndromes [9–11,41–43]. A meta-analysis by Jaarsma et al. comprising a total of 13,741 patients who underwent SPECT and 1319 patients evaluated by ^{82}Rb PET showed that PET provides a higher specificity (81% vs 61%, $P < .05$), while sensitivity was comparable between these two nuclear imaging techniques at a per-patient level [9]. Similar findings were also reported by Mc Ardle and colleagues in a meta-analysis evaluating the diagnostic performance of ^{82}Rb PET and SPECT [10]. In contrast to the prior results, both sensitivity (90% vs 85%) and specificity (88% vs 85%) of ^{82}Rb PET was shown to be superior to SPECT MPI using invasive coronary angiography (ICA) as a reference standard. In the majority of prior studies, the difference in accuracy in favor of PET MPI was mainly driven by a lower rate of false positive findings, which is attributed to the higher image resolution and routine availability of accurate attenuation correction. Unlike in SPECT, attenuation correction is mandatory for PET due to the coincidence effect and the resulting photon attenuation. Indeed, a meta-analysis conducted by Huang et al. revealed a notably heightened specificity (80% vs 68%, $P < .05$) of MPI with the application of attenuation correction, while the sensitivity remained unaltered (84% vs 80%) [44]. Also, when using gated PET MPI, considering non-perfusion variables like the change in LV ejection fraction (LVEF) during pharmacological stress provides relevant diagnostic information, as a lower LVEF reserve (LVEF stress − LVEF rest) has been associated with high-risk anatomical features and the extent of ischemia [45,46].

Nevertheless, the majority of stress MPI methods have been assessed for their diagnostic performance against an ICA reference standard. When refereed against fractional flow reserve (FFR), PET achieved a substantially better sensitivity (84% vs 74%) and specificity (87% vs 79%) than SPECT for discerning the hemodynamic significance of epicardial lesions [11]. However, it is important to highlight that while ^{82}Rb stands as the prevailing radionuclide employed in PET for myocardial perfusion assessment, [^{15}O]H_2O PET has undergone the most rigorous validation against FFR [47]. Indeed, in the meta-analysis by Takx et al., the sole three PET studies that employed FFR as the gold standard utilized [^{15}O]H_2O as perfusion tracer [11]. Additionally, a significant portion of the studies faced limitations due to a design where the comparison between imaging methods was conducted indirectly. In contrast, the Prospective Comparison of Cardiac PET/CT, SPECT/CT Perfusion Imaging and CT Coronary Angiography With Invasive Coronary Angiography (PACIFIC-1) study conducted a direct head-to-head analysis of CCTA, SPECT, and [^{15}O]H_2O PET MPI in symptomatic individuals without a documented cardiac history [43]. Routine FFR measurements were employed as the reference standard revealing outcomes consistent with earlier studies. PET MPI demonstrated a significantly superior diagnostic accuracy compared to SPECT MPI (85% vs 77%, $P = .003$) and CCTA (85%

Table 2. Summary results of meta-analysis assessing the diagnosis performance of PET, SPECT, and CMR for diagnosing Coronary Artery Disease.

Study	Year	PET						SPECT						CMR						Reference standard
		Per − Patient			Per − Vessel			Per − Patient			Per − Vessel			Per − Patient			Per − Vessel			
		N°	Sen (%)	Spe (%)	N°	Sen (%)	Spe (%)	N°	Sen (%)	Spe (%)	N°	Sen (%)	Spe (%)	N°	Sen (%)	Spe (%)	N°	Sen (%)	Spe (%)	
Mc Ardle [10]	2012	1344	90	88	–	–	–	1755	85	85	–	–	–	–	–	–	–	–	–	ICA
Jaarsma [9]	2012	762	84	81	888	77	88	13,508	88	61	13,545	45	79	2483	89	76	2121	84	83	ICA
Takx [11]	2015	224	84	87	870	83	89	533	74	79	924	61	84	798	89	87	1830	87	91	FFR
Danad [40]	2017	–	–	–	–	–	–	110	70	78	470	57	75	70	90	94	371	91	85	FFR
Yang [41]	2019	–	–	–	1572	83	89	842	72	79	1235	64	89	614	87	87	2134	85	89	FFR
Xu [42]	2021	3647	87	86	–	80	86	22,563	86	74	–	71	84	4969	88	81	–	83	86	ICA or FFR

CMR, Cardiac Magnetic Resonance; *FFR*, Fractional Flow Reserve; *ICA*, Invasive Coronary Angiography; *PET*, Positron Emission Tomography; *Sen*, Sensitivity; *Spe*, Specificity; *SPECT*, Single Photon Emission Computed Tomography.

vs 74%, $P = .02$). Notably, the sensitivity of SPECT consistently proved to be lower in detecting hemodynamically significant CAD, as indicated by FFR, in comparison to the more widely adopted ICA standard. The pooled sensitivity and specificity of SPECT MPI for the detection of hemodynamically significant CAD as defined by FFR ranged from 70%–74% and 78%–79%, respectively [11,40,41]. Furthermore, in challenging populations, such as those with a history of prior CAD, MPI typically demonstrates reduced diagnostic effectiveness. This can be explained by a greater prevalence of multi-vessel disease, diffuse CAD, and coronary microvascular disease (CMVD). In a recent study, 189 patients with a history of CAD were evaluated using a head-to-head design comparing SPECT, [^{15}O]H_2O PET, and CMR MPI [48]. Overall, PET yielded a higher diagnostic accuracy (75%) than SPECT (65%, $P = .03$) and CMR (64%, $P = .05$) and a significantly higher discrimination ability (c-statistic = .80) compared to SPECT (c-statistic = .66, $P = .001$) and CMR (c-statistic = .67, $P = .001$). As it relates to detection of obstructive CAD in patients without a prior history, PET and CMR demonstrate comparable diagnostic value as first line test (Table 2). Notably, a recent study compared the performance of ^{82}Rb PET and CMR as second-line tests in diagnosing hemodynamically significant CAD in a group of 372 patients with suspected obstructive coronary disease based on CCTA [49]. The study demonstrated a higher diagnostic accuracy for ^{82}Rb PET (78% vs 73%, $P = .03$).

Reports employing [^{13}N]NH_3 as a perfusion tracer are less abundant but indicate a comparable performance [50,51]. Of interest is the recent introduction of [^{18}F]Flurpiridaz as a perfusion tracer. Despite its promising characteristics, [^{18}F]Flurpiridaz made a somewhat hesitant introduction into the clinical arena. In the first phase III trial, [^{18}F]Flurpiridaz PET showed better overall discriminatory capacity than SPECT, however it did not meet the prespecified non-inferiority threshold for specificity [52]. Sensitivity and specificity for [^{18}F]Flurpiridaz PET MPI was 71.9% and 76.2%, respectively. The recently published second phase III trial met the primary outcome for accuracy in detecting CAD (60% predefined threshold for sensitivity and specificity) and also the secondary outcome of higher accuracy than SPECT [53]. Maddahi et al. found sensitivity of [^{18}F]Flurpiridaz PET to be significantly higher than SPECT (80.3% vs 68.7%, $P < .01$), while specificity was not inferior and numerically superior (specificity 63.8% vs 61.7%, $P < .01$ for non-inferiority) in favor of [^{18}F]Flurpiridaz PET. However, its acceptance and approval have been postponed due to ambiguous results from the first phase III trial, as the rate of false-positive findings hindered achieving the prespecified specificity criteria. This may be attributed to the lack of an appropriate reference standard, utilizing an invasive anatomical reference instead of a functional one, which may have predominantly impacted sensitivity and, to a lesser extent, specificity. Moreover, non-optimal imaging protocols due to the lack of respiratory and cardiac gating may have hampered accurate co-registration. In addition, quantification could have provided further insights and may have revealed whether the observed positive findings were concomitant with pathological stress MBF. The low specificity observed in both phase III trials may have resulted from heterogeneity of stress perfusion (in the normal ranges of stress MBF), a physiological phenomenon which may resemble the appearance of a perfusion defect on relative tracer uptake images. A similar phenomenon is seen for [^{15}O]H_2O PET, which requires an alternative interpretation of visual images. The use of quantification in [^{15}O]H_2O PET MPI provides additional diagnostic value, not only by reducing the number of false-negative findings, but also by providing insight into the mechanism of `reduced´ perfusion seen on qualitative images. There is mounting evidence suggesting that the addition of absolute flow values enhances diagnostic accuracy of myocardial perfusion imaging for the detection of flow-limiting CAD [54–56].

CLINICAL CHALLENGES OF QUANTITATIVE PET MYOCARDIAL PERFUSION IMAGING

Unlike qualitative assessments, which rely on visual interpretation, PET facilitates quantification of myocardial perfusion in absolute terms. Several studies support the diagnostic advantages of quantitative PET imaging by improving diagnostic accuracy (Table 3) [55–63]. There are a number of clinical scenarios in which quantitative PET provides additional information over relative MPI imaging alone. Although truly balanced ischemia is rare, it is a condition that goes undetected by the evaluation of relative tracer uptake imaging and its identification is improved by quantitative PET [58,61,64–66]. In addition, qualitative imaging underestimates the severity of ischemia in patients with multivessel ischemic disease, as the region with the highest perfusion, despite being within the pathological range, is assumed to represent a reference area with normal perfusion when using a qualitative approach. As such, relative MPI is not well-suited to serve as a guide for coronary revascularization but merely functions as a gatekeeper to the

catheterization laboratory. Moreover, quantitative MBF imaging allows for the detection of CMVD which often leads to a homogeneous decrease in MBF, which may be disguised by a qualitative assessment [67]. Furthermore, quantification may also aid in distinguishing heterogeneous stress perfusion, a physiological phenomenon, from a true perfusion defect (see section above).

However, it should be recognized that quantitative PET allows for the generation of multiple myocardial perfusion parameters. That said, stress MBF and myocardial flow reserve (MFR), which is the ratio of stress to rest MBF, are the most frequently used perfusion metrics. The reliance of MFR on resting perfusion renders it less accurate than stress MBF, since a reduction in MFR is not necessarily concomitant with reduced stress flow but might also be caused by an increased resting MBF. Under resting conditions, baseline flow is auto regulated in response to metabolic demand and therefore also strongly relates to heart rate and blood pressure [57]. Indeed, stress MBF is a better mean for defining hemodynamic significant CAD as reflected by abnormal FFR achieving a significantly higher accuracy (86% vs 78% for MFR $P < .01$) mainly driven by a lower rate of false positive findings [47]. The superior accuracy of stress MBF over MFR has been confirmed in several studies, paving the way for stress only protocols [56,58,68,69]. However, the choice for hyperemic MBF or MFR depends on the utilized tracer and its kinetics. For example, the low extraction fraction of ^{82}Rb resulting in a non-linear relationship between MBF and uptake ratio requires additional corrections, especially at high flow rates, to account for this phenomenon (Figure 2). These corrections inevitably come with a penalty of increased noise and a subsequent suboptimal quantification of MBF (Figure 2B). While a relatively good correlation between hyperemic MBF quantification with [^{15}O]H_2O and ^{82}Rb exist, broad limits of agreement between the measurements have been reported [39,70]. Consequently, the sole reliance on hyperemic MBF for ^{82}Rb might provide different results in comparison to the other flow tracers that are characterized by a high extraction fraction ([^{13}N]NH_3, [^{18}F]Flurpiridaz and [^{15}O]H_2O) and a K_1 proportional to MBF. Even though PET MBF quantification using the same method shows robustness with relatively low test-retest variability (coeficients of variation ~20%), the computed flow values vary significantly depending on the kinetic model employed in each software [71,72]. Therefore, when reporting quantitative PET data, it is crucial to describe technical aspects such as the hardware, tracer, software, and kinetic model used, as these factors affect the final results [21,27,73,74].

Partly due to the aforementioned reasons, establishing a cut-off value to differentiate between normal and pathological MBF has proven challenging. This issue is illustrated in Table 4 which enumerates the various cut-off values reported in the literature [47,56–59,62,68,75–91]. Of

Table 3. Improvements in diagnostic performance for Coronary Artery Disease using Quantitative PET.

Author	Year	Tracer	Reference standard	Comparison	Metric	Qualitative PET	Strategy with quantitative PET	P-value
Kajander [55]	2011	[^{15}O]H_2O	FFR ≤ .8	Relative Perfusion vs Regional stress MBF	Accuracy	73%	92%	–
Fiechter [57]	2012	[^{13}N]Ammonia	ICA > 50%	Relative Perfusion vs Relative Perfusion + Global MFR	Accuracy	79%	92%	P < .01
Hajjiri [58]	2009	[^{13}N]Ammonia	ICA ≥ 70%	Relative Perfusion vs Regional stress MBF	Accuracy	72%	84%	P < .01
Lee [56]	2016	[^{13}N]Ammonia	FFR ≤ .8	Relative Perfusion vs Relative Perfusion + Regional MFR	NRI	Ref.	.629	P < .01
Kuronuma [59]	2024	^{82}Rubidium	ICA ≥ 70%	Relative Perfusion vs Relative Perfusion + Regional stress MBF	c-statistic	.78	.82	P = .02
Packard [60]	2022	[^{18}F]Flurpiridaz	ICA > 50%	Relative Perfusion vs Relative Perfusion + Regional stress MBF	c-statistic	.73	.77	P < .05

FFR, Fractional Flow Reserve; *ICA*, Invasive Coronary Angiography; *NRI*, Net reclassification index; *Ref.*, Reference.

note, for [^{15}O]H_2O PET imaging, a cut-off value of less than 2.3 mL/min/g has been established to effectively differentiate between ischemic and non-ischemic myocardial regions. This well-defined threshold, is based on findings from a study characterized by its prospective design and significant population size, with FFR serving as the reference standard [47]. Crucially, it appears that different clinical scenarios warrant the application of varying cut-offs. In a recently published study 172 symptomatic coronary artery bypass graft patients were examined by [^{15}O]H_2O PET and showed a cut-off value of 1.53 mL/min/g to predict coronary revascularization by PCI, while a stress flow of 1.85 mL/min/g (both on a per-vessel level) was found to predict relief of angina after revascularization therapy [81]. Furthermore, it has been proposed to establish age- and sex-specific cut-off values, considering that females and young individuals physiologically exhibit higher MBF values compared to their counterparts [82,92–94].

THE DIFFERENCE BETWEEN MYOCARDIAL BLOOD FLOW AND FRACTIONAL FLOW RESERVE

Although the use of cut-off values seems insurmountable in daily clinical practice, a problem that arises when defining a threshold for ischemia is that it fails to grasp the complexity of the ischemic heart disease spectrum, confining myocardial perfusion to a binary phenomenon. Also, the use of an ICA or FFR reference standard with a binary cut-off for defining disease implies that there is a threshold at which point the benefit of a treatment suddenly appears or disappears, while every measure of perfusion or anatomical severity of CAD is continuous by nature. Moreover, FFR and MBF are only crudely related, since FFR reflects only the functional repercussions of epicardial atherosclerosis, while PET MPI allows for the measurement of the net impact of epicardial atherosclerosis (focal and diffuse) and the coronary microvasculature on myocardial perfusion. Therefore, the disagreement of FFR and PET MBF imaging does not reflect the failure of either technique, but is merely the resultant of a different ischemic syndrome phenotypes. More importantly, by the nature of the kinetic flow models, PET derived MBF is expressed in mL/min/g, taking into account the myocardial mass subtended by a given epicardial artery. On the other hand, FFR provides an intracoronary pressure gradient, which is primarily influenced by epicardial stenoses and, to a lesser extent, by myocardial mass, since intracoronary gradients are also governed by coronary flow, which scales with myocardial mass [95]. Therefore, FFR is not an effective tool for quantifying the downstream myocardial mass at risk. For instance, a FFR $\leq$ .8 in a large artery or a proximal stenosis holds more significant clinical implications than the same FFR value for a small artery or distal lesion. On the other hand, PET lacks information on lesion-specific ischemia in the presence of serial stenoses, while with a drawback of the pressure wire may identify the lesion with the highest pressure drop amenable for revascularization [96]. Another challenge for PET MPI in guiding revascularizations is CMVD leading to erroneous interpretations for decision-making for revascularization therapy. The use of the relative flow reserve (RFR), ratio of hyperemic flow in the (most) ischemic vascular territory to normal flow in a reference area, nullifies the impact of CMVD, which is thought to be a homogeneous process taking an equal toll on the whole myocardium. In a study by Stuijfzand et al., RFR had a slightly higher accuracy (82% vs 74% for hyperemic MBF, P = NS) for predicting FFR defined hemodynamic significant lesions, driven by a high specificity (98% vs 70% for hyperemic MBF) [97]. Nevertheless, the correlation with FFR was only moderate (r = .44; $P < .001$). Of note, the correlation between change of MBF and FFR following revascularization appears stronger (r = .63, $P < .01$) [98]. In 130 symptomatic patients evaluated by [^{13}N]NH_3 PET, the use of RFR (optimal cut-off in the study by Lee et al. .82) as a perfusion metric was associated with the highest accuracy for the detection of myocardial ischemia as defined by FFR (82% vs 76% for stress MBF) and provided incremental diagnostic information beyond visual perfusion defect assessment, stress MBF and MFR [56]. Figure 3 presents a clinical case illustrating discordance between FFR and PET-derived MBF measurements, highlighting how both elements can contribute to the clinical decision-making process for the management of CAD.

PROGNOSTIC VALUE OF MYOCARDIAL PERFUSION ASSESSED BY PET

The presence of a normal non-invasive imaging test in patients with suspected CAD suggests a low likelihood of adverse events, indicating a favorable prognosis. According to a comprehensive meta-analysis conducted by Smulders and colleagues, the annual event rates associated with a normal non-invasive imaging test (including CMR, stress echocardiography [SE], SPECT and PET) differed from those seen following a negative CCTA [99]. The variability in event rates was not solely due to the inherent characteristics of the tests, but rather reflected the demographics of the studied population and the prevalence of CAD. In fact, the annual event rate showed a positive correlation with the

Table 4. Different proposed PET MPI quantitative thresholds for defining Coronary artery disease.

	Author	Year	N° patients (vessels/territories)	Stress MBF Cut-off (mL/min/g)	MFR cut-off	Reference
[^{15}O]H_2O	Nesterov [75]	2009	48	2.5	–	ICA
	Kajander [76]	2010	107 (312)	2.5	–	ICA or FFR in intermediate lesions
	Danad [77]	2013	120 (360)	1.86	2.3	ICA, FFR in a subset of vessels
	Thomassen [78]	2013	44 (132)	2.2	–	ICA
	Joutsiniemi [68]	2014	104 (312)	2.4	2.5	ICA or FFR in intermediate lesions
	Danad [79]	2014	66 (198)	2.2	2.5	FFR
	Danad [47]	2014	330 (860)	2.3	2.5	FFR
	Berti [80]	2016	77	2.05	–	ICA or FFR in intermediate lesions
	Vester [81]	2023	24 (21)	1.85	2.11	Symptom relief after revascularization
	Hoek [82]	2024	560	Male = 2.3 Female = 2.8	Male = 2.7 Female = 2.6	FFR
[^{13}N]Ammonia	Muzik [83]	1998	51	1.52	2.74	ICA
	Hajjiri [58]	2009	48 (144)	1.85	2	ICA
	Fiechter [57]	2012	73	–	2	ICA
	Morton [84]	2012	41	–	1.44	ICA
	Lee [56]	2016	130 (307)	1.99	2.12	FFR
	Berti [80]	2016	42	1.79	2.06	ICA or FFR in intermediate lesions
^{82}Rubidium	Anagnostopoulos [85]	2008	22 [39]	1.7	2	ICA
	Ziadi [86]	2011	704	–	2	Prognosis
	Johnson [87]	2011	1674	.91	1.74	PET relative defect and stress ST changes/ angina
	Naya [88]	2013	901	–	2	Prognosis
	Naya [62]	2014	290	–	1.93	ICA
	Kuronuma [59]	2024	341	2	2	ICA
	Rasmussen [89]	2024	400	2.13	2	FFR
[^{18}F]Flurpiridaz	Packard [90]	2020	245 (735)	1.6	2.5	ICA
	Otaki [91]	2022	231 (693)	1.81	2.31	ICA

FFR, Fractional Flow Reserve; *ICA*, Invasive Coronary Angiography; *MBF*, Myocardial Blood Flow; *MFR*, Myocardial Flow Reserve.

overall event risk of the studied population ($r = .726$, $P < .001$) [99]. After adjustment for event rates and CAD prevalence, the pooled annualized rate of cardiac death and MI following a negative result showed no significant difference between CCTA and other stress tests, as illustrated in Figure 4.

The prognostic significance of the extension and severity of stress perfusion defects with conventional qualitative PET MPI is widely acknowledged [100–102]. Despite variations in patient groups, outcome definitions, and follow-up periods across studies, the consensus remains consistent: a normal scan typically indicates a lower risk of cardiac events (< ~1% per year, Figure 4), while an abnormal scan suggests a higher risk of future cardiovascular events, with the degree of risk correlating with the extent and severity of observed ischemia. The predictive capacity for cardiovascular outcomes significantly improves when PET is used to quantify myocardial perfusion instead of relying on relative perfusion images. Incorporating hyperemic MBF or MFR has been shown to enhance prognostication, even among patients without regional perfusion abnormalities [86,103,104]. Patients with abnormal MBF, even in the absence of obstructive epicardial CAD, exhibit increased rates of non-fatal MI, cardiovascular death, and all-cause mortality attributed to CMVD [105,106]. A recent meta-analysis evaluating the prognostic role of PET MFR in patients with suspected or known CAD, encompassing 13 different studies with a total of 11,864 participants and a follow-up period of up to 7.1 years, found a HR of 1.93 (95% CI: 1.65-2.27) for

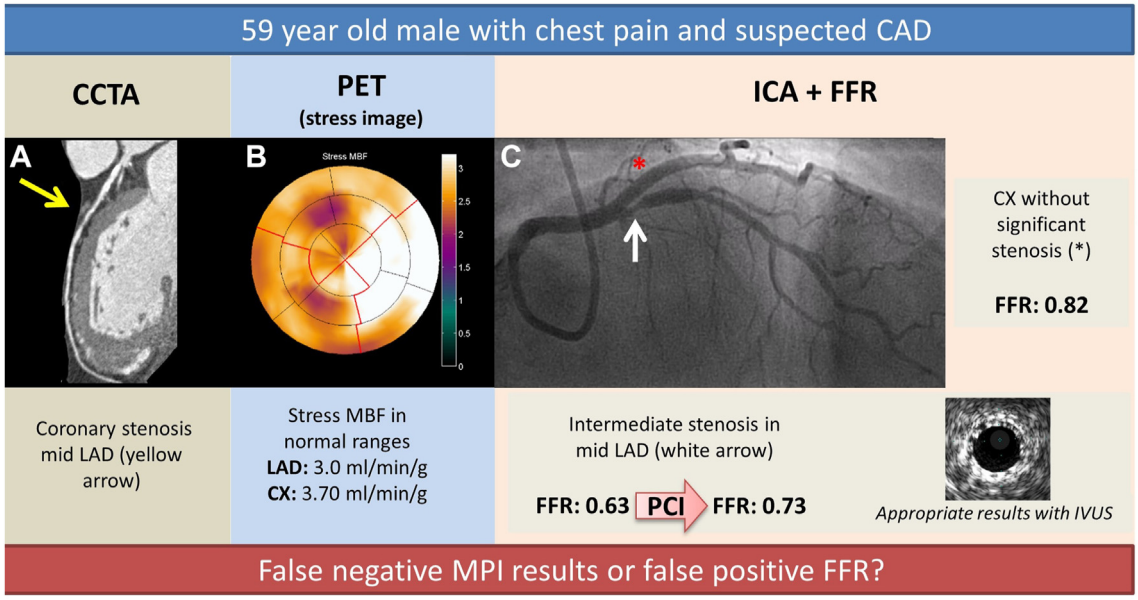

Figure 3. Clinical case: Discordance between PET perfusion and invasive functional findings. A 59-year-old man with no relevant medical history was referred for chest pain workup. He agreed to participate in a comparative non-invasive imaging study protocol for which he underwent [^{15}O]H_2O PET, and CCTA prior to invasive coronary angiography. CCTA displayed a stenosis in the left anterior descending artery (LAD) (A). PET quantitative perfusion polar map was generated (B). Although well within normal limits, hyperemic myocardial blood flow and flow reserve (not shown in the figure) were attenuated in the LAD perfusion territory (3.0 mL/min/g and 3.5, respectively) as compared with the circumflex territory (3.70 mL/min/g and 4.2, respectively) in a dominant left coronary artery. Invasive coronary angiography subsequently demonstrated an intermediate lesion of the LAD (C). FFR was significantly reduced in the LAD (.63) but also borderline impaired in the circumflex (.82). After percutaneous coronary intervention, including verification of appropriate stent apposition with intravascular ultrasound, FFR increased to .73. Due to lack of additional focal obstructive lesions, no further percutaneous treatment was employed. The patient has remained free from symptoms during a year follow-up period. The current case displays a combination of seemingly discordant results from invasive and non-invasive techniques. Particularly the normal myocardial perfusion imaging with quantitative PET in the presence of an epicardial coronary lesion deemed significant with FFR, raises the question which imaging modality failed to correctly identify the hemodynamic severity of the coronary lesion. A more detailed analysis, however, provides support for the notion that all of the results can in fact be matched and should be considered concordant. Even though PET derived hyperemic myocardial blood flow was within normal limits, attenuated stress flow was observed in the LAD vascular territory (3.0 mL/min/g in the stenotic area compared with 3.7 mL/min/g in the circumflex territory). Based on the linear relationship between hyperemic perfusion and driving pressure, theoretical hyperemic myocardial blood flow in the absence of any pressure drop along the epicardial coronary artery would be 4.76 mL/min/g in the LAD territory (1/.63 x 3.0 mL/min/g), which is in the higher range of physiological hyperemic flow values. This value is in concordance with the potential hyperemic flow in the circumflex area where FFR was reduced due to diffuse coronary atherosclerosis (1/.82 x 3.7 = 4.5 mL/min/g). The combination of these data illustrates that FFR measurements can be severely depressed in the presence of relatively preserved hyperemic myocardial blood flow and flow reserve. The underlying physiological basis for these findings is the relatively low minimal coronary vascular resistance of the microvascular bed in this particular patient. The key question, whether an epicardial coronary lesion with a significant hyperemic pressure drop in the presence of relatively preserved perfusion results in ischemia, remains unanswered as perfusion imaging and FFR solely document metabolic supply and do not take myocardial demand into account, the misbalance of which ultimately results in ischemia. It does, however, suggest that FFR thresholds for revascularization may be individually determined and are dependent on the condition of the microvascular bed. Interrogation of a coronary lesion by the combination of FFR and quantitative perfusion assessment may therefore act complementary and more comprehensively guide treatment strategy.

major adverse cardiac events (including cardiac death, MI, hospitalization, late revascularization and heart failure) in the group with the lowest global MFR [107]. Most studies utilized ^{82}Rb (with three [^{13}N]NH_3 studies) as the perfusion agent, employing various MFR thresholds ranging from <1.6 to < 2. It is important to note that the prognostic value of global MFR remains significant even after adjusting for factors such as clinical risk, extension of CAD by ICA, coronary artery calcium (CAC) score, or the severity and extent of qualitative perfusion deficit (Figure 5A) [86,103,106,108–111,116].

While most prognosis insights stem from MFR as the predictor, hyperemic MBF along with other quantitative metrics are also considered outcome predictors (Figure 5B) [107,108,110,112–115]. Despite some conflicting evidence, it appears that MFR) and MBF offer complementary prognostic information [115,117]. Interestingly, MFR, unlike MBF, includes resting perfusion, which serves as a marker influenced by factors such as

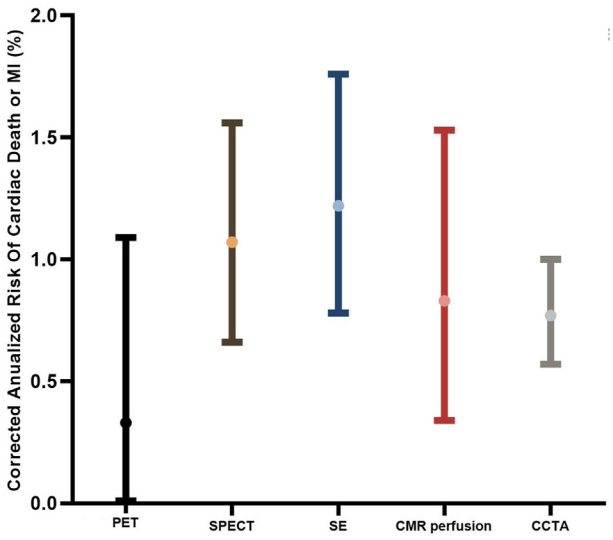

Figure 4. Cardiovascular risk associated with a negative results of a non-invasive image test. Pooled annualized event rates for cardiac death and myocardial infarction after a negative test result of non-invasive cardiac investigations, adjusted for population event risk and prevalence of CAD. Absence of significant difference was found between negative CCTA and the others tests. Adapted from Smulders et al. [99] PET, positron emission tomography; SPECT, single photon emission computed tomography; SE, stress echocardiography; CMR, cardiac magnetic resonance; CCTA, coronary computed tomography angiography.

hypertension and age. In theory, this should broaden the scope of prognostic information available, thereby offering a more comprehensive risk assessment. Nevertheless, in a study conducted by Bom et al. utilizing [^{15}O]H_2O PET, only hyperemic MBF emerged as a significant predictor for MI and all-cause mortality following adjustment for clinical risk factors and both quantitative perfusion metrics [112]. Furthermore, there is convincing evidence that the physiological severity of ischemia, as determined by the affected amount of myocardium, provides valuable information regarding future adverse events. The concept known as `ischemic burden´, the percentage of the LV with inducible ischemia, has proven useful in identifying individuals who could potentially benefit from revascularization in terms of outcomes. It has been established, through SPECT studies, that $\geq$ 10% ischemic burden of the LV is associated with a reduction in MI and death following revascularization therapy as opposed to medical therapy alone [118]. In a retrospective study using [^{15}O]H_2O PET, an ischemic burden of $\geq$24% based upon stress MBF was shown to confer prognostic value (prediction of non-fatal MI and death) beyond clinical characteristics and even MFR [113]. In a large observational study including 16,029 patients undergoing ^{82}Rb PET MPI with a follow-up of 3.7 years, a lower threshold was established than the previously reported threshold for SPECT [119]. In this study, a PET defined ischemic burden of 5% was associated to a potential survival benefit following early revascularization therapy.

INCREMENTAL PROGNOSTIC VALUE OF PET MPI OVER CT

A recent study by Jukema et al. demonstrated that among patients with suspected CAD, the absence of regional quantitative perfusion abnormalities was associated with prolonged periods of freedom from adverse outcomes (death and non-fatal MI) [105]. This effect was evident across patients with no CAD, non-obstructive CAD, and obstructive CAD as defined by CCTA. In a separate study, a machine learning methodology that integrated clinical, CCTA, and PET data demonstrated PET's ability to enhance predictive capabilities for adverse events over a 4-year follow-up period, while this effect disappeared after 4 years [120]. This finding suggests that ischemia may be linked to an increased risk of events in the short term, while anatomical indicators of atherosclerosis offer risk information on the long term. However, there is conflicting data regarding whether MBF imaging possesses prognostic value beyond anatomical indices of coronary atherosclerosis. In a study by Driessen et al., diameter stenosis and high risk plaque features were predictive of non-fatal MI and death, while abnormal hyperemic MBF ($<$ 2.3 mL/min/g derived from [^{15}O]H_2O PET) was not independently associated with adverse events [121]. Conversely, Maaniitty and colleagues showed that [^{15}O]H_2O PET provided additional prognostic information for predicting non-fatal MI and unstable angina in patients with obstructive CAD identified on CCTA [122]. However, PET was not independently linked to all-cause mortality after adjusting for the presence of obstructive CAD on CCTA. A recently published study showed that visually and automatically determined CAC scoring from low-dose CT scans have an incremental prognostic value, irrespective from the [^{15}O]H_2O PET results. If added to PET, CAC further improved the prediction of future adverse events [123].

EXPLORING THE MORPHO-FUNCTIONAL SUBSTRATE OF ISCHEMIC SYNDROMES WITH QUANTITATIVE PET MPI

Alterations in myocardial flow detected by PET could result from focal coronary stenoses, diffuse atherosclerosis, or CMVD. Although, mostly

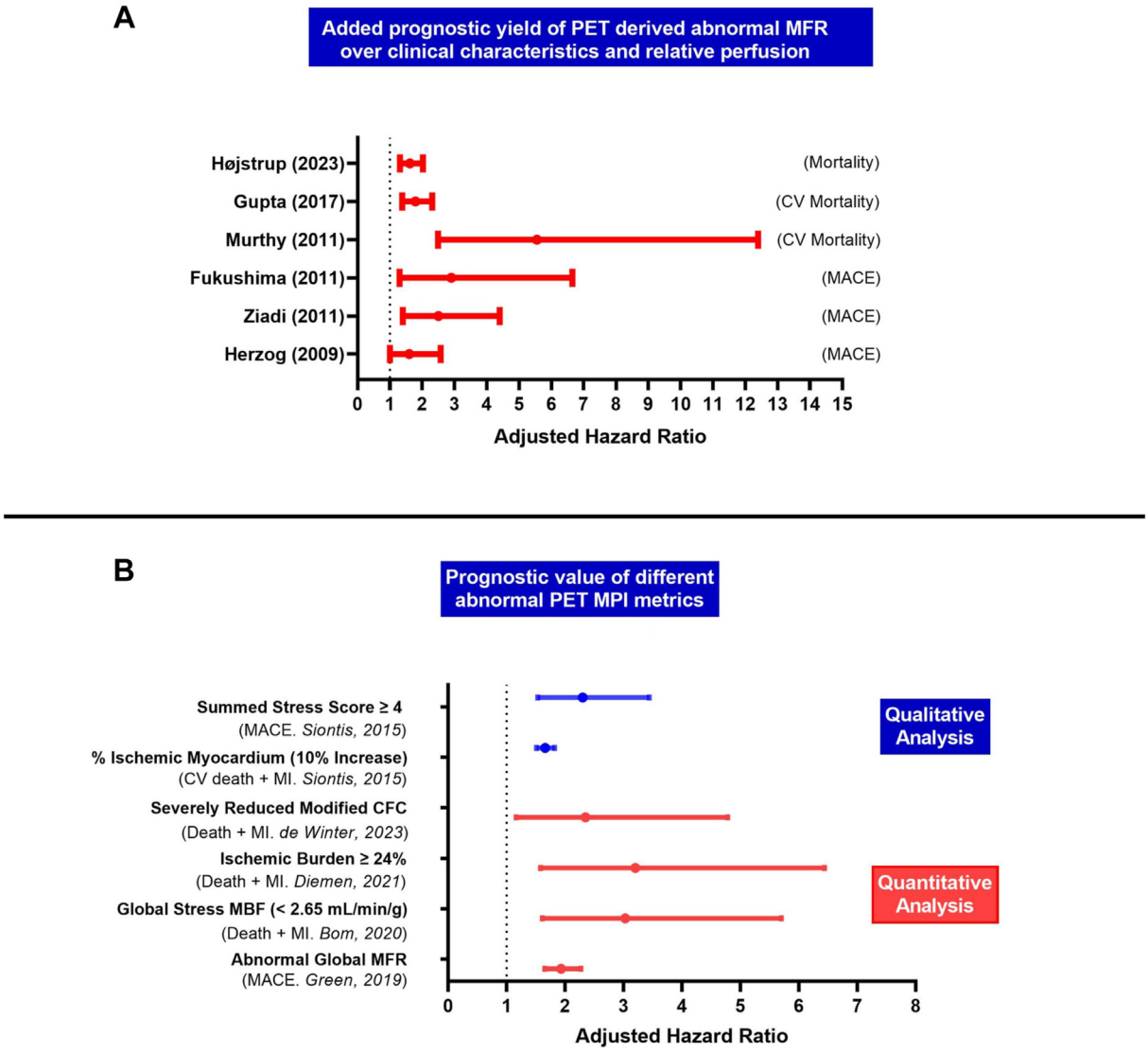

Figure 5. Prognostic value of PET MPI. (A) Different studies reporting the hazard ratio of abnormal PET MFR adjusted by clinical variables and by the extension of quantitative perfusion defect (B) Adjusted hazard ratio for different PET MPI metrics derived from qualitative and quantitative analysis [86,107–115]. MACE, major adverse cardiac events; MI, myocardial infarction; CV, cardiovascular.

investigated with ^{82}Rb PET, the integration of complementary continuous metrics (hyperemic MBF and MFR) into coronary flow capacity (CFC) mapping creates a robust framework for visualization of PET perfusion data (See Figure 6 for further description) [5,124]. By enhancing this visual representation with specific coronary physiology concepts and incorporating the valuable insights from the CAC score, we can disentangle these potential diagnoses and determine the main drivers of ischemia in an individual patient, something currently unachievable with other non-invasive methods. In this regard, other PET MPI derived indices might provide additional diagnostic insights, such as the assessment of longitudinal perfusion gradients [125–128]. Longitudinal perfusion gradients have been proposed as a useful tool to differentiate between predominantly focal disease, characterized by a sudden drop in perfusion beyond the expected level of stenosis in a designated vascular territory, and diffuse epicardial disease, marked by a gradual decrease in perfusion from the basal to the apical segments (Figure 7) [127,129]. Identifying these distinct phenotypes of chronic coronary syndromes is crucial, as observational data suggest that diffuse CAD is linked to a worse prognosis despite revascularization, and the advantages of revascularization in this context are uncertain [130,131]. Furthermore, due to the high spatial resolution of PET, it is possible to evaluate both relative and quantitative myocardial perfusion across the myocardial wall, allowing the identification of subendocardial ischemia [79,132–134]. It has been suggested that relative subendocardial to subepicardial ischemia during

vasodilator stress can be explained by the presence of diffuse epicardial disease coupled with adequate microvascular function [135]. Although these analyses have the potential to differentiate CMVD from diffuse CAD, further validation is needed [136].

HYBRID IMAGING

There is ongoing debate regarding the clinical value of hybrid imaging in patients with suspected CAD. Although the prognostic implications of incorporating anatomy to perfusion have already been discussed in this document, uncertainty remains about the additional diagnostic value of hybrid imaging for significant CAD. The PACIFIC-1 trial revealed that the information provided by CCTA does not improve the already high diagnostic performance of PET in detecting FFR-defined significant lesions, with accuracies of 84% and 85%, respectively ($P = .82$) [43]. This has been supported by a comprehensive meta-analysis, including studies employing different MPI methods (PET, SPECT, and CMR), which show a marginal benefit in accuracy for the hybrid approach [137]. These data are further supported by the Danish study of Non-Invasive testing in Coronary Artery Disease (Dan-NICAD) study demonstrating a dramatic decline in sensitivity of SPECT (36%) and CMR perfusion imaging (41%) conducted subsequent to a positive CCTA scan in patients lacking a prior history of CAD [138].

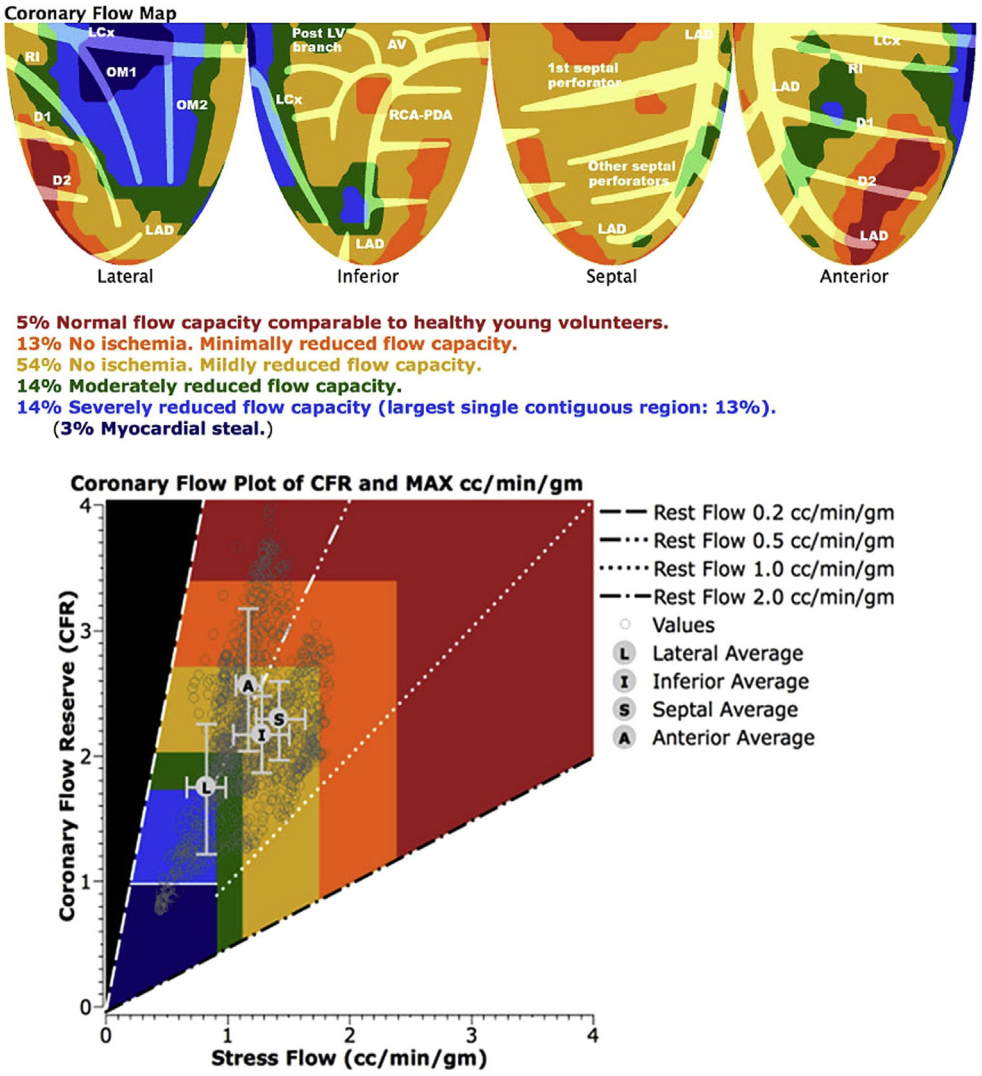

Figure 6. Coronary flow capacity mapping. In this CFC framework, each pixel of left ventricle volume is assigned with its respective values of stress MBF and MFR. These pixels are then plotted on a nomogram (bottom), with stress MBF and MFR on its axes, and with bands of different colors that delineate the different levels within the perfusion spectrum (from red in normal to blue in ischemic). These colored pixels are then visually displayed in 4-quadrant map of the left ventricle (top), with coronary anatomical references also depicted to guide interpretation. Adapted from Gould et al. [5] AV, atrioventricular nodal artery; D, diagonal branch; LAD, left anterior descending artery; LCx, left circumflex artery; LV, left ventricular; OM, obtuse marginal. PDA, posterior descending artery; RCA, right coronary artery; RI, ramus intermedius.

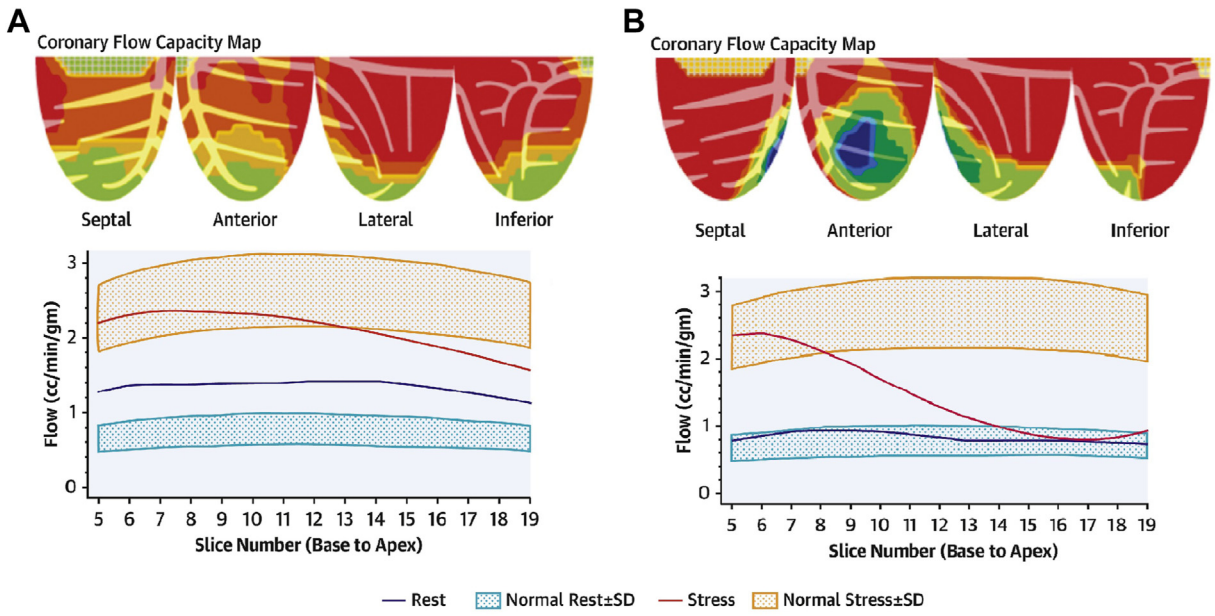

Figure 7. (A) Gradual base to apex longitudinal perfusion gradient and CFC maps of a patient with mild diffuse coronary narrowing. (B) Regional severe stress perfusion abnormality indicative of severe focal stenosis with transmural ischemia. Adapted from Gould et al. [127] CFC, coronary flow caap

Presumably, this involves navigating the threshold of 50% stenosis in CCTA, resulting in an increased frequency of misinterpretations. Indeed, a study by Meijboom et al. showed the highest rates of overestimation and underestimation clustered around the cut-off value of 50% [139]. The frequency of misclassification is inherently influenced the percentage of patients with `intermediate stenosis´ and as such subsequently influenced by the disease prevalence of the studied population. The findings become even more ambiguous with the integration of perfusion imaging in these intricate intermediate lesions, likely also residing on the boundary between normal and abnormal myocardial perfusion. This introduces an additional dimension of uncertainty to result interpretation. Several other diagnostic tests have demonstrated a poor performance around a discriminatory cut-off. Particularly noteworthy are the recently unveiled findings from real-world clinical data regarding the application of FFR-CT in the United Kingdom, which revealed a positive predictive value (PPV) of merely 49% for FFR-CT in patients with intermediate stenosis (50%–69%) [140].

The CAC score, a simple and reproducible anatomical measure indicative of the total atherosclerotic burden, is a powerful tool for patient risk stratification that incorporates prognostic information to PET MPI results [123,141–143]. It can be derived from low-dose ungated CT attenuation correction scans, available in all contemporary PET/CT systems. Previous studies have demonstrated a good correlation between visually estimated and qualitative CAC scores derived from attenuation correction scans and those obtained from dedicated CAC scans [144–146]. Recent evidence reveals that new deep learning models can compute CAC scores from non-gated CT scans in a short period of time (< 10 seconds), offering a CAC score that predicts risk comparably to standard CAC scores [143]. Chest pain guidelines provide a class 2a indication for the addition of CAC to the stress test in patients without known CAD [147].

THE ROLE OF QUANTITATIVE PET IN ISCHEMIC SYNDROMES AFTER THE ISCHEMIA TRIAL

Subsequent to the publication of the ISCHEMIA trial, some have questioned the role of MPI in stratifying individual patient risk and guiding interventional therapy. This stems from the observation that ischemia-guided revascularization did not markedly alter hard outcomes, even in populations identified as being at `high´ risk of events [148]. However, categorizing the ISCHEMIA trial results as neutral is a matter of debate and such claims require careful consideration. First, the results of this trial demonstrated that the patients randomized to the invasive group had lower rates of type 1 MI compared to the conservative arm [149]. Furthermore, an extended follow-up to a median of 5.7 years revealed a significant reduction in cardiovascular death in the invasive strategy arm (adjusted HR = .78 [95% CI: .63-.96]), with no observed differences in all-cause mortality [150].

In the contemporary era of highly effective guideline-directed medical therapy as the backbone of CAD management, these findings are somehow unexpected. Nevertheless, there are other aspects that might have attenuated the impact of revascularization in this trial. First, patient selection was based on non-sensitive techniques like SPECT, SE, and exercise-ECG (in the 25% of the participants). Moreover, only about half of the patients included in the trial had severe ischemia and approximately 60% of these patients were classified using less accurate methods, namely exercise-ECG and SE, in which the interaction between revascularization and ischemia severity on prognosis has not been extensively studied [148]. All the above, combined with a 23% crossover from the conservative arm to revascularization, might partially account for the dampened but still positive impact of revascularization on MI and cardiovascular mortality outcomes. As previously shown, evidence derived from well conducted observational research has identified interaction between extent of ischemia defined by PET and the effectiveness of revascularization in predicting major cardiovascular events [117,119,151]. It is plausible to hypothesize that the use of this more accurate imaging technique could facilitate the identification of high-risk individuals who would benefit from revascularization in terms of hard cardiovascular outcomes.

On the contrary, there is less dispute regarding the effectiveness of revascularization in alleviating symptoms and improving quality of life, as consistent evidence supports this claim [152]. Previous studies have demonstrated that the burden of ischemic symptoms correlates with the severity of hypoperfusion measured by PET scans [153]. Patients in this category are expected to experience significant symptom relief following revascularization, primarily due to the restoration of myocardial blood flow post-procedure [81,98,154–156]. As highlighted earlier, a comprehensive PET MPI assessment can reveal both the anatomical and functional origins of symptoms. Patients with CMD can be identified, classified, and their response to treatment can be assessed with control images [157]. Additionally, PET MPI enables the detection of relative subendocardial ischemia as the underlying cause of angina in patients with diffuse non-severe epicardial disease, a condition commonly overlooked by conventional imaging methods [133].

PET MPI IN CARDIOMYOPATHIES

Cardiomyopathy and heart failure patients, with either reduced or preserved ejection fraction, can exhibit reduced myocardial perfusion. This can result from different mechanisms, including CMVD or the coexistence with obstructive CAD [158–163]. The role of CMVD in non-ischemic cardiomyopathies is not fully unraveled; and it remains uncertain whether CMVD is a causal factor or merely a consequence of the primary disease [164,165]. Of note, epicardial CAD is frequently observed in patients with hypertrophic cardiomyopathy (HCM), and heart failure with preserved ejection fraction (HFpEF) [166–168]. In this context, careful interpretation of quantitative perfusion metrics is necessitated, as global reduction in these could be secondary to CMVD or diffuse CAD. In that line, we suggest complementing the interpretation of PET MPI with metrics of relative perfusion such as RFR. In patients with HCM, increased wall thickness has been associated with reduced global stress MBF [169]. Furthermore, subendocardial ischemia identified by PET has been linked to decreased LVEF reserve under vasodilator stress [163]. A recent observational study involving 1255 patients with LVEF $\leq$ 40% found that an attenuated global MFR was associated with a higher risk of mortality (adjusted HR = 1.08, $P < .01$ per .1 unit decrease), even after adjustment for clinical factors, left ventricular function, and the extent of perfusion defects [170]. Notably, there was no interaction between MFR and the ethiology of cardiomyopathy, whether ischemic or non-ischemic [170]. Additionally, PET MPI can be used non-invasively to diagnose cardiac allograft vasculopathy and the presence of low global perfusion has been shown as an independent predictor of all-cause mortality in heart transplant patients [171–173].

FUTURE PERSPECTIVES

A significant issue that arises when utilizing the PET is the abundance of tracers and the diversity in cut-off values for ischemia documented in literature (Table 4). To further develop this technique and reinforce its analytical strength and replicability of subsequent investigations, it is fundamental to generate consensus within cardiac imaging community. Currently, the only tracer that has achieved this level of acceptance, with multiple software validations and a firmly established cut-off value, is $[^{15}O]H_2O$ in patients without known CAD [27]. In order to definitively address the long-lasting and somewhat unresolved question regarding the efficacy of revascularization in preventing major adverse cardiac events within chronic coronary syndromes, it is imperative to conduct a randomized trial including patients with severe ischemia,

meticulously selected with PET MPI. Moreover, incorporating comparative arms of the study with optimal medical therapy, PET-guided management, and FFR-directed invasive approach could provide more definitive insights into the most accurate strategy. An ongoing randomized trial is currently investigating the role of CFC derived from PET MPI in directing the multidisciplinary treatment of patients with stable or highly suspected CAD compared to the conventional approach (CENTURY trial, NCT00756379) [174]. For cardiologists it is paramount to grasp the full potential of this technique, understanding its wide range of uses that extend beyond conventional qualitative perfusion. It is clear that the strength of this technique lies in the integration of the immense amount of information it provides. However, relying exclusively on the mental integration of different PET metrics may be insufficient. As deep learning continues to advance innovative prognostic models will emerge that not only take maximum advantage of the data produced, but also convey more meaningful messages to clinicians to inform clinical decision-making.

CONCLUSIONS

The use of PET MPI specially with flow quantification markedly enriches the diagnostic and risk stratification capacities in chronic coronary syndrome patients. Non-invasive flow quantification provides a detailed and unparalleled source of information that, until now, has been largely underutilized in traditional clinical practice. As the availability and popularity of this technique increase, it is imperative for cardiologists to familiarize themselves with its novel applications and interpretations. In this context, the role of cardiac imaging experts becomes indispensable. Assisted by their experience, we can unfold the full potential of the PET MPI integration in diagnosis and tailored personalized care.

FUNDING AND SUPPORT

This study did not receive funding.

DISCLOSURES

The authors declare the following financial interests/personal relationships which may be considered as potential competing interests: Hendrik J. Harms reports a relationship with MedTrace that includes: employment. If there are other authors, they declare that they have no known competing financial interests or personal relationships that could have appeared to influence the work reported in this paper.

REFERENCES

[1] Newby DE, Adamson PD, Berry C, Boon NA, Dweck MR, Flather M, et al. Coronary CT angiography and 5-year risk of myocardial infarction. N Engl J Med 2018;379:924–33.

[2] Douglas Pamela S, Hoffmann U, Patel Manesh R, Mark Daniel B, Al-Khalidi Hussein R, Cavanaugh B, et al. Outcomes of anatomical versus functional testing for coronary artery disease. N Engl J Med 2105;372:1291–300. https://doi.org/10.1056/NEJMoa1415516.

[3] Shaw LJ, Berman DS, Maron DJ, Mancini GB, Hayes SW, Hartigan PM, et al. Optimal medical therapy with or without percutaneous coronary intervention to reduce ischemic burden: results from the Clinical Outcomes Utilizing Revascularization and Aggressive Drug Evaluation (COURAGE) trial nuclear substudy. Circulation 2008;117:1283–91.

[4] Reynolds HR, Shaw LJ, Min JK, Page CB, Berman DS, Chaitman BR, et al. Outcomes in the ISCHEMIA trial based on coronary artery disease and ischemia severity. Circulation 2021;144:1024–38.

[5] Gould KL, Johnson NP, Bateman TM, Beanlands RS, Bengel FM, Bober R, et al. Anatomic versus physiologic assessment of coronary artery disease. Role of coronary flow reserve, fractional flow reserve, and positron emission tomography imaging in revascularization decision-making. J Am Coll Cardiol 2013;62:1639–53.

[6] Schindler TH, Schelbert HR, Quercioli A, Dilsizian V. Cardiac PET imaging for the detection and monitoring of coronary artery disease and microvascular health. JACC Cardiovasc Imaging 2010;3:623–40.

[7] Reeves RA, Halpern EJ, Rao VM. Cardiac imaging trends from 2010 to 2019 in the medicare population. Radiol Cardiothorac Imag 2021;3:e210156.

[8] Advisory Board. The 3 market dynamics affecting CV imaging. 2019. https://www.advisory.com/blog/2019/02/cv-imaging.

[9] Jaarsma C, Leiner T, Bekkers SC, Crijns HJ, Wildberger JE, Nagel E, et al. Diagnostic performance of noninvasive myocardial perfusion imaging using single-photon emission computed tomography, cardiac magnetic resonance, and positron emission tomography imaging for the detection of obstructive coronary artery disease: a meta-analysis. J Am Coll Cardiol 2012;59:1719–28.

[10] Mc Ardle BA, Dowsley TF, deKemp RA, Wells GA, Beanlands RS. Does rubidium-82 PET have superior accuracy to SPECT perfusion imaging for the diagnosis of obstructive coronary disease?: a systematic review and meta-analysis. J Am Coll Cardiol 2012;60:1828–37.

[11] Takx RA, Blomberg BA, El Aidi H, Habets J, de Jong PA, Nagel E, et al. Diagnostic accuracy of stress myocardial perfusion imaging compared to invasive coronary angiography with fractional flow reserve meta-analysis. Circ Cardiovasc Imag 2015;8.

[12] Gould KL, Schelbert HR, Phelps ME, Hoffman EJ. Noninvasive assessment of coronary stenoses with myocardial perfusion imaging during pharmacologic coronary vasodilatation. V. Detection of 47 percent diameter coronary stenosis with intravenous nitrogen-13 ammonia and emission-computed tomography in intact dogs. Am J Cardiol 1979;43:200–8.

[13] Schelbert HR, Wisenberg G, Phelps ME, Gould KL, Henze E, Hoffman EJ, et al. Noninvasive assessment of coronary stenoses by myocardial imaging during pharmacologic coronary vasodilation. VI. Detection of coronary artery disease in human beings with intravenous N-13 ammonia and positron computed tomography. Am J Cardiol 1982;49:1197–207.

[14] Wisenberg G, Schelbert HR, Hoffman EJ, Phelps ME, Robinson GD, Selin CE, et al. In vivo quantitation of regional myocardial blood flow by positron-emission computed tomography. Circulation 1981;63:1248–58.
[15] Klein R, Beanlands RS, deKemp RA. Quantification of myocardial blood flow and flow reserve: technical aspects. J Nucl Cardiol 2010;17:555–70.
[16] Nakazato R, Berman DS, Alexanderson E, Slomka P. Myocardial perfusion imaging with PET. Imag Med 2013;5:35–46.
[17] Moody JB, Lee BC, Corbett JR, Ficaro EP, Murthy VL. Precision and accuracy of clinical quantification of myocardial blood flow by dynamic PET: a technical perspective. J Nucl Cardiol 2015;22:935–51.
[18] Dilsizian V, Bacharach SL, Beanlands RS, Bergmann SR, Delbeke D, Dorbala S, et al. ASNC imaging guidelines/SNMMI procedure standard for positron emission tomography (PET) nuclear cardiology procedures. J Nucl Cardiol 2016;23:1187–226.
[19] Winther S, Dupont Rasmussen L, Westra J, Abdulzahra SRK, Dahl JN, Gormsen LC, et al. Danish study of Non-Invasive Testing in Coronary Artery Disease 3 (Dan-NICAD 3): study design of a controlled study on optimal diagnostic strategy. Open Heart 2023;10.
[20] Di Carli MF, Gormsen LC, Chareonthaitawee P, Johnson GB, Beanlands R, DeKemp R, et al. Rationale and design of the RAPID-WATER-FLOW trial: radiolabeled perfusion to identify coronary artery disease using water to evaluate responses of myocardial FLOW. J Nucl Cardiol 2024;31:101779.
[21] Murthy VL, Bateman TM, Beanlands RS, Berman DS, Borges-Neto S, Chareonthaitawee P, et al. Clinical quantification of myocardial blood flow using PET: joint position paper of the SNMMI cardiovascular council and the ASNC. J Nucl Cardiol. 2018 Feb;25(1):269–97. https://doi.org/10.1007/s12350-017-1110-x.
[22] Partridge M, Spinelli A, Ryder W, Hindorf C. The effect of $\beta+$ energy on performance of a small animal PET camera. Nucl Instrum Methods Phys Res Sect A Accel Spectrom Detect Assoc Equip 2006;568:933–6.
[23] Mullani NA, Goldstein RA, Gould KL, Marani SK, Fisher DJ, O'Brien Jr HA, et al. Myocardial perfusion with rubidium-82. I. Measurement of extraction fraction and flow with external detectors. J Nucl Med 1983;24:898–906.
[24] Goldstein RA, Mullani NA, Marani SK, Fisher DJ, Gould KL, O'Brien Jr HA. Myocardial perfusion with rubidium-82. II. Effects of metabolic and pharmacologic interventions. J Nucl Med 1983;24:907–15.
[25] Donato L, Bartolomei G, Federighi G, Torreggiani G. Measurement of coronary blood flow by external counting with radioactive rubidium. Critical appraisal and validation of the method. Circulation 1966;33:708–18.
[26] Bergmann SR, Fox KA, Rand AL, McElvany KD, Welch MJ, Markham J, et al. Quantification of regional myocardial blood flow in vivo with H215O. Circulation 1984;70:724–33.
[27] Sciagrà R, Lubberink M, Hyafil F, Saraste A, Slart R, Agostini D, et al. EANM procedural guidelines for PET/CT quantitative myocardial perfusion imaging. Eur J Nucl Med Mol Imag 2021;48:1040–69.
[28] Harms HJ, Knaapen P, de Haan S, Halbmeijer R, Lammertsma AA, Lubberink M. Automatic generation of absolute myocardial blood flow images using [15O]H2O and a clinical PET/CT scanner. Eur J Nucl Med Mol Imag 2011;38:930–9.
[29] Lubberink M, Harms HJ, Halbmeijer R, de Haan S, Knaapen P, Lammertsma AA. Low-dose quantitative myocardial blood flow imaging using 15O-water and PET without attenuation correction. J Nucl Med 2010;51:575–80.
[30] Bravo PE, Chien D, Javadi M, Merrill J, Bengel FM. Reference ranges for LVEF and LV volumes from electrocardiographically gated ^{82}Rb cardiac PET/CT using commercially available software. J Nucl Med 2010;51:898–905.
[31] Chander A, Brenner M, Lautamäki R, Voicu C, Merrill J, Bengel FM. Comparison of measures of left ventricular function from electrocardiographically gated ^{82}Rb PET with contrast-enhanced CT ventriculography: a hybrid PET/CT analysis. J Nucl Med 2008;49:1643–50.
[32] Hattori N, Bengel FM, Mehilli J, Odaka K, Ishii K, Schwaiger M, et al. Global and regional functional measurements with gated FDG PET in comparison with left ventriculography. Eur J Nucl Med 2001;28:221–9.
[33] Nordström J, Kero T, Harms HJ, Widström C, Flachskampf FA, Sörensen J, et al. Calculation of left ventricular volumes and ejection fraction from dynamic cardiac-gated 15O-water PET/CT: 5D-PET. EJNMMI Physics 2017;4:26.
[34] Nordström J, Kvernby S, Kero T, Sörensen J, Harms HJ, Lubberink M. Left-ventricular volumes and ejection fraction from cardiac ECG-gated 15O-water positron emission tomography compared to cardiac magnetic resonance imaging using simultaneous hybrid PET/MR. J Nucl Cardiol 2023;30:1352–62.
[35] Iida H, Rhodes CG, de Silva R, Yamamoto Y, Araujo LI, Maseri A, et al. Myocardial tissue fraction–correction for partial volume effects and measure of tissue viability. J Nucl Med 1991;32:2169–75.
[36] Yamamoto Y, de Silva R, Rhodes CG, Araujo LI, Iida H, Rechavia E, et al. A new strategy for the assessment of viable myocardium and regional myocardial blood flow using 15O-water and dynamic positron emission tomography. Circulation 1992;86:167–78.
[37] de Haan S, Harms HJ, Lubberink M, Allaart CP, Danad I, Chen WJ, et al. Parametric imaging of myocardial viability using ^{15}O-labelled water and PET/CT: comparison with late gadolinium-enhanced CMR. Eur J Nucl Med Mol Imag 2012;39:1240–5.
[38] Timmer SAJ, Teunissen PFA, Danad I, Robbers L, Raijmakers P, Nijveldt R, et al. In vivo assessment of myocardial viability after acute myocardial infarction: a head-to-head comparison of the perfusable tissue index by PET and delayed contrast-enhanced CMR. J Nucl Cardiol 2017;24:657–67.
[39] Hoff CM, Sørensen J, Kero T, Bouchelouche K, Harms HJ, Frøkiær J, et al. Quantitative and qualitative comparison of Rubidium-82 and Oxygen-15 water cardiac PET. J Nucl Cardiol 2024:101796.
[40] Danad I, Szymonifka J, Twisk JWR, Norgaard BL, Zarins CK, Knaapen P, et al. Diagnostic performance of cardiac imaging methods to diagnose ischaemia-causing coronary artery disease when directly compared with fractional flow reserve as a reference standard: a meta-analysis. Eur Heart J 2017;38:991–8.
[41] Yang K, Yu S-Q, Lu M-J, Zhao S-H. Comparison of diagnostic accuracy of stress myocardial perfusion imaging for detecting hemodynamically significant coronary artery disease between cardiac magnetic resonance and nuclear medical imaging: a meta-analysis. Int J Cardiol 2019;293:278–85.
[42] Xu J, Cai F, Geng C, Wang Z, Tang X. Diagnostic performance of CMR, SPECT, and PET imaging for the identification of coronary artery disease: a meta-analysis. Front Cardio Med 2021;8.
[43] Danad I, Raijmakers PG, Driessen RS, Leipsic J, Raju R, Naoum C, et al. Comparison of coronary CT angiography, SPECT, PET, and hybrid imaging for diagnosis of

ischemic heart disease determined by fractional flow reserve. JAMA Cardiol 2017;2:1100–7.
[44] Huang JY, Huang CK, Yen RF, Wu HY, Tu YK, Cheng MF, et al. Diagnostic performance of attenuation-corrected myocardial perfusion imaging for coronary artery disease: a systematic review and meta-analysis. J Nucl Med 2016;57:1893–8.
[45] Dorbala S, Vangala D, Sampson U, Limaye A, Kwong R, Di Carli MF. Value of vasodilator left ventricular ejection fraction reserve in evaluating the magnitude of myocardium at risk and the extent of angiographic coronary artery disease: a 82Rb PET/CT study. J Nucl Med 2007;48:349–58.
[46] Hsiao E, Ali B, Blankstein R, Skali H, Ali T, Bruyere Jr J, et al. Detection of obstructive coronary artery disease using regadenoson stress and 82Rb PET/CT myocardial perfusion imaging. J Nucl Med 2013;54:1748–54.
[47] Danad I, Uusitalo V, Kero T, Saraste A, Raijmakers PG, Lammertsma AA, et al. Quantitative assessment of myocardial perfusion in the detection of significant coronary artery disease: cutoff values and diagnostic accuracy of quantitative [(15)O]H2O PET imaging. J Am Coll Cardiol 2014;64:1464–75.
[48] Driessen RS, van Diemen PA, Raijmakers PG, Knuuti J, Maaniitty T, Underwood SR, et al. Functional stress imaging to predict abnormal coronary fractional flow reserve: the PACIFIC 2 study. Eur Heart J 2022;43:3118–28.
[49] Rasmussen LD, Winther S, Eftekhari A, Karim SR, Westra J, Isaksen C, et al. Second-line myocardial perfusion imaging to detect obstructive stenosis: head-to-head comparison of CMR and PET. J Am Coll Cardiol 2023;16:642–55.
[50] Husmann L, Wiegand M, Valenta I, Gaemperli O, Schepis T, Siegrist PT, et al. Diagnostic accuracy of myocardial perfusion imaging with single photon emission computed tomography and positron emission tomography: a comparison with coronary angiography. Int J Cardiovasc Imag 2008;24:511–8.
[51] Fathala A, Aboulkheir M, Shoukri MM, Alsergani H. Diagnostic accuracy of (13)N-ammonia myocardial perfusion imaging with PET-CT in the detection of coronary artery disease. Cardiovasc Diagn Ther 2019;9:35–42.
[52] Maddahi J, Lazewatsky J, Udelson JE, Berman DS, Beanlands RSB, Heller GV, et al. Phase-III clinical trial of fluorine-18 flurpiridaz positron emission tomography for evaluation of coronary artery disease. J Am Coll Cardiol 2020;76:391–401.
[53] Maddahi J, Agostini D, Bateman Timothy M, Bax Jeroen J, Beanlands Rob SB, Berman Daniel S, et al. Flurpiridaz F-18 PET myocardial perfusion imaging in patients with suspected coronary artery disease. J Am Coll Cardiol 2023;82:1598–610.
[54] Yoshinaga K, Katoh C, Manabe O, Klein R, Naya M, Sakakibara M, et al. Incremental diagnostic value of regional myocardial blood flow quantification over relative perfusion imaging with generator-produced rubidium-82 PET. Circ J 2011;75:2628–34.
[55] Kajander SA, Joutsiniemi E, Saraste M, Pietilä M, Ukkonen H, Saraste A, et al. Clinical value of absolute quantification of myocardial perfusion with (15)O-water in coronary artery disease. Circ Cardiovasc Imag 2011;4:678–84.
[56] Lee JM, Kim CH, Koo B-K, Hwang D, Park J, Zhang J, et al. Integrated myocardial perfusion imaging diagnostics improve detection of functionally significant coronary artery stenosis by 13N-ammonia positron emission tomography. Circul Cardio Imag 2016;9:e004768.
[57] Fiechter M, Ghadri JR, Gebhard C, Fuchs TA, Pazhenkottil AP, Nkoulou RN, et al. Diagnostic value of 13N-ammonia myocardial perfusion PET: added value of myocardial flow reserve. J Nucl Med 2012;53:1230–4.
[58] Hajjiri Mohammad M, Leavitt Marcia B, Zheng H, Spooner Amy E, Fischman Alan J, Gewirtz H. Comparison of positron emission tomography measurement of adenosine-stimulated absolute myocardial blood flow versus relative myocardial tracer content for physiological assessment of coronary artery stenosis severity and location. J Am Coll Cardiol 2009;2:751–8.
[59] Keiichiro K, Chih-Chun W, Ananya S, Mark L, Sean WH, Yuka O, et al. Automated motion correction for myocardial blood flow measurements and diagnostic performance of ^{82}Rb PET myocardial perfusion imaging. J Nucl Med 2024;65:139.
[60] Packard RRS, Votaw JR, Cooke CD, Van Train KF, Garcia EV, Maddahi J. 18F-flurpiridaz positron emission tomography segmental and territory myocardial blood flow metrics: incremental value beyond perfusion for coronary artery disease categorization. Eur Heart J Cardiovasc Imag 2022;23:1636–44.
[61] Ziadi MC, Dekemp RA, Williams K, Guo A, Renaud JM, Chow BJ, et al. Does quantification of myocardial flow reserve using rubidium-82 positron emission tomography facilitate detection of multivessel coronary artery disease? J Nucl Cardiol 2012;19:670–80.
[62] Naya M, Murthy VL, Taqueti VR, Foster CR, Klein J, Garber M, et al. Preserved coronary flow reserve effectively excludes high-risk coronary artery disease on angiography. J Nucl Med 2014;55:248–55.
[63] Moody JB, Poitrasson-Rivière A, Hagio T, Buckley C, Weinberg RL, Corbett JR, et al. Added value of myocardial blood flow using (18)F-flurpiridaz PET to diagnose coronary artery disease: the flurpiridaz 301 trial. J Nucl Cardiol 2021;28:2313–29.
[64] Aarnoudse WH, Botman KJ, Pijls NH. False-negative myocardial scintigraphy in balanced three-vessel disease, revealed by coronary pressure measurement. Int J Cardiovasc Inter 2003;5:67–71.
[65] Masanao N, Venkatesh LM, Viviany RT, Courtney RF, Josh K, Mariya G, et al. Preserved coronary flow reserve effectively excludes high-risk coronary artery disease on angiography. J Nucl Med 2014;55:248.
[66] Maaniitty T, Stenström I, Saraste A, Knuuti J. Extensive and balanced reduction of myocardial blood flow in patients with suspected obstructive coronary artery disease: 15O-water PET study. Int J Cardiol 2021;338:1–7.
[67] Schindler TH, Fearon WF, Pelletier-Galarneau M, Ambrosio G, Sechtem U, Ruddy TD, et al. Myocardial perfusion PET for the detection and reporting of coronary microvascular dysfunction: a JACC: cardiovascular imaging expert panel statement. J Am Coll Cardiol 2023;16:536–48.
[68] Joutsiniemi E, Saraste A, Pietilä M, Mäki M, Kajander S, Ukkonen H, et al. Absolute flow or myocardial flow reserve for the detection of significant coronary artery disease? Europ Heart J Cardio Imag 2014;15:659–65.
[69] Ibrahim D, Pieter GR, Yolande EA, Hendrik JH, Stefan de H, Mijntje LPVDO, et al. Hybrid imaging using quantitative $H_2{}^{15}O$ PET and CT-based coronary angiography for the detection of coronary artery disease. J Nucl Med 2013;54:55.
[70] Prior JO, Allenbach G, Valenta I, Kosinski M, Burger C, Verdun FR, et al. Quantification of myocardial blood flow with 82Rb positron emission tomography: clinical validation with 15O-water. Eur J Nucl Med Mol Imag 2012;39:1037–47.

[71] Nesterov SV, Deshayes E, Sciagrà R, Settimo L, Declerck JM, Pan XB, et al. Quantification of myocardial blood flow in absolute terms using (82)Rb PET imaging: the RUBY-10 Study. JACC Cardiovasc Imag 2014;7:1119–27.
[72] Sdringola S, Johnson NP, Kirkeeide RL, Cid E, Gould KL. Impact of unexpected factors on quantitative myocardial perfusion and coronary flow reserve in young, asymptomatic volunteers. JACC Cardiovasc Imag 2011;4:402–12.
[73] Chareonthaitawee P, Bateman T, Beanlands R, Berman D, Calnon D, Di Carli M, et al. Atlas for reporting PET myocardial perfusion imaging and myocardial blood flow in clinical practice: an information statement from the American Society of Nuclear Cardiology. J Nucl Cardiol 2023;30.
[74] Tilkemeier PL, Bourque J, Doukky R, Sanghani R, Weinberg RL. ASNC imaging guidelines for nuclear cardiology procedures : standardized reporting of nuclear cardiology procedures. J Nucl Cardiol 2017;24:2064–128.
[75] Nesterov SV, Han C, Mäki M, Kajander S, Naum AG, Helenius H, et al. Myocardial perfusion quantitation with 15O-labelled water PET: high reproducibility of the new cardiac analysis software (Carimas). Eur J Nucl Med Mol Imag 2009;36:1594–602.
[76] Kajander S, Joutsiniemi E, Saraste M, Pietilä M, Ukkonen H, Saraste A, et al. Cardiac positron emission tomography/computed tomography imaging accurately detects anatomically and functionally significant coronary artery disease. Circulation 2010;122:603–13.
[77] Danad I, Raijmakers PG, Appelman YE, Harms HJ, de Haan S, van den Oever ML, et al. Hybrid imaging using quantitative H215O PET and CT-based coronary angiography for the detection of coronary artery disease. J Nucl Med 2013;54:55–63.
[78] Thomassen A, Petersen H, Diederichsen ACP, Mickley H, Jensen LO, Johansen A, et al. Hybrid CT angiography and quantitative 15O-water PET for assessment of coronary artery disease: comparison with quantitative coronary angiography. Eur J Nucl Med Mol Imag 2013;40:1894–904.
[79] Danad I, Raijmakers PG, Harms HJ, Heymans MW, van Royen N, Lubberink M, et al. Impact of anatomical and functional severity of coronary atherosclerotic plaques on the transmural perfusion gradient: a [15O]H2O PET study. Eur Heart J 2014;35:2094–105.
[80] Berti V, Sciagrà R, Neglia D, Pietilä M, Scholte AJ, Nekolla S, et al. Segmental quantitative myocardial perfusion with PET for the detection of significant coronary artery disease in patients with stable angina. Eur J Nucl Med Mol Imag 2016;43:1522–9.
[81] Vester M, Madsen S, Kjærulff MLG, Tolbod LP, Nielsen BRR, Kristensen SD, et al. Myocardial perfusion imaging by (15)O-H(2)O positron emission tomography predicts clinical revascularization procedures in symptomatic patients with previous coronary artery bypass graft. Eur Heart J Open 2023;3:oead044.
[82] Hoek R, van Diemen PA, Raijmakers PG, Driessen RS, Somsen YBO, de Winter RW, et al. Determining hemodynamically significant coronary artery disease: patient-specific cutoffs in quantitative myocardial blood flow using [(15)O]H(2)O PET imaging. J Nucl Med 2024;65(7):1113–21.
[83] Muzik O, Duvernoy C, Beanlands RSB, Sawada S, Dayanikli F, Wolfe ER, et al. Assessment of diagnostic performance of quantitative flow measurements in normal subjects and patients with angiographically documented coronary artery disease by means of nitrogen-13 ammonia and positron emission tomography. J Am Coll Cardiol 1998;31:534–40.
[84] Morton G, Chiribiri A, Ishida M, Hussain ST, Schuster A, Indermuehle A, et al. Quantification of absolute myocardial perfusion in patients with coronary artery disease: comparison between cardiovascular magnetic resonance and positron emission tomography. J Am Coll Cardiol 2012;60:1546–55.
[85] Anagnostopoulos C, Almonacid A, El Fakhri G, Curillova Z, Sitek A, Roughton M, et al. Quantitative relationship between coronary vasodilator reserve assessed by 82Rb PET imaging and coronary artery stenosis severity. Eur J Nucl Med Mol Imag 2008;35:1593–601.
[86] Ziadi MC, deKemp RA, Williams KA, Guo A, Chow BJW, Renaud JM, et al. Impaired myocardial flow reserve on rubidium-82 positron emission tomography imaging predicts adverse outcomes in patients assessed for myocardial ischemia. J Am Coll Cardiol 2011;58:740–8.
[87] Johnson NP, Gould KL. Physiological basis for angina and ST-segment change: PET-verified thresholds of quantitative stress myocardial perfusion and coronary flow reserve. J Am Coll Cardiol 2011;4:990–8.
[88] Naya M, Murthy VL, Foster CR, Gaber M, Klein J, Hainer J, et al. Prognostic interplay of coronary artery calcification and underlying vascular dysfunction in patients with suspected coronary artery disease. J Am Coll Cardiol 2013;61:2098–106.
[89] Rasmussen LD, Gormsen LC, Ejlersen JA, Karim SR, Westra J, Knudsen LL, et al. Impact of absolute myocardial blood flow quantification on the diagnostic performance of PET-based perfusion scans using (82)Rubidium. Circ Cardiovasc Imag 2024;17:e016138.
[90] Rene P, John V, Charles C, Kenneth Van T, Ernest G, Jamshid M. strong>Diagnostic performance of automated myocardial blood flow quantitation by flurpiridaz F18 positron emission tomography: a sub-study of the flurpiridaz F18 301 clinical trial</strong&gt. J Nucl Med 2020;61:652.
[91] Otaki Y, Van Kriekinge SD, Wei CC, Kavanagh P, Singh A, Parekh T, et al. Improved myocardial blood flow estimation with residual activity correction and motion correction in (18)F-flurpiridaz PET myocardial perfusion imaging. Eur J Nucl Med Mol Imag 2022;49:1881–93.
[92] Nickander J, Themudo R, Sigfridsson A, Xue H, Kellman P, Ugander M. Females have higher myocardial perfusion, blood volume and extracellular volume compared to males - an adenosine stress cardiovascular magnetic resonance study. Sci Rep 2020;10:10380.
[93] Danad I, Raijmakers PG, Appelman YE, Harms HJ, de Haan S, van den Oever ML, et al. Coronary risk factors and myocardial blood flow in patients evaluated for coronary artery disease: a quantitative [15O]H2O PET/CT study. Eur J Nucl Med Mol Imag 2012;39:102–12.
[94] Chareonthaitawee P, Kaufmann PA, Rimoldi O, Camici PG. Heterogeneity of resting and hyperemic myocardial blood flow in healthy humans. Cardiovasc Res 2001;50:151–61.
[95] Johnson NP, Gould KL. How do PET myocardial blood flow reserve and FFR differ? Current cardiology. Reports 2020;22:20.
[96] Nijjer SS, Sen S, Petraco R, Mayet J, Francis DP, Davies JER. The Instantaneous wave-Free Ratio (iFR) pullback: a novel innovation using baseline physiology to optimise coronary angioplasty in tandem lesions. Cardiovasc Revascul Med 2015;16:167–71.
[97] Stuijfzand WJ, Uusitalo V, Kero T, Danad I, Rijnierse MT, Saraste A, et al. Relative flow reserve derived from quantitative perfusion imaging may not outperform stress myocardial blood flow for identification of

hemodynamically significant coronary artery disease. Circul Cardio Imag 2015;8:e002400.
[98] Jukema RA, de Winter RW, Hopman L, Driessen RS, van Diemen PA, Appelman Y, et al. Impact of cardiac history and myocardial scar on increase of myocardial perfusion after revascularization. Eur J Nucl Med Mol Imag 2023;50:3897–909.
[99] Smulders MW, Jaarsma C, Nelemans PJ, Bekkers S, Bucerius J, Leiner T, et al. Comparison of the prognostic value of negative non-invasive cardiac investigations in patients with suspected or known coronary artery disease-a meta-analysis. Eur Heart J Cardiovasc Imag 2017;18:980–7.
[100] Lertsburapa K, Ahlberg AW, Bateman TM, Katten D, Volker L, Cullom SJ, et al. Independent and incremental prognostic value of left ventricular ejection fraction determined by stress gated rubidium 82 PET imaging in patients with known or suspected coronary artery disease. J Nucl Cardiol 2008;15:745–53.
[101] Yoshinaga K, Chow BJW, Williams K, Chen L, deKemp RA, Garrard L, et al. What is the prognostic value of myocardial perfusion imaging using rubidium-82 positron emission tomography? J Am Coll Cardiol 2006;48:1029–39.
[102] Dorbala S, Hachamovitch R, Curillova Z, Thomas D, Vangala D, Kwong RY, et al. Incremental prognostic value of gated Rb-82 positron emission tomography myocardial perfusion imaging over clinical variables and rest LVEF. J Am Coll Cardiol 2009;2:846–54.
[103] Murthy VL, Naya M, Foster CR, Hainer J, Gaber M, Di Carli G, et al. Improved cardiac risk assessment with noninvasive measures of coronary flow reserve. Circulation 2011;124:2215–24.
[104] Farhad H, Dunet V, Bachelard K, Allenbach G, Kaufmann PA, Prior JO. Added prognostic value of myocardial blood flow quantitation in rubidium-82 positron emission tomography imaging. Eur Heart J Cardiovasc Imaging 2013;14:1203–10.
[105] Jukema R, Maaniitty T, van Diemen P, Berkhof H, Raijmakers PG, Sprengers R, et al. Warranty period of coronary computed tomography angiography and [15O]H2O positron emission tomography in symptomatic patients. Europ Heart J Cardio Imag 2023;24:304–11.
[106] Miller RJH, Han D, Singh A, Pieszko K, Slomka PJ, Gransar H, et al. Relationship between ischaemia, coronary artery calcium scores, and major adverse cardiovascular events. Eur Heart J Cardiovasc Imag 2022;23:1423–33.
[107] Green R, Cantoni V, Acampa W, Assante R, Zampella E, Nappi C, et al. Prognostic value of coronary flow reserve in patients with suspected or known coronary artery disease referred to PET myocardial perfusion imaging: a meta-analysis. J Nucl Cardiol 2021;28:904–18.
[108] Gupta A, Taqueti VR, van de Hoef TP, Bajaj NS, Bravo PE, Murthy VL, et al. Integrated noninvasive physiological assessment of coronary circulatory function and impact on cardiovascular mortality in patients with stable coronary artery disease. Circulation 2017;136:2325–36.
[109] Højstrup S, Hansen KW, Talleruphuus U, Marner L, Bjerking L, Jakobsen L, et al. Myocardial flow reserve, an independent prognostic marker of all-cause mortality assessed by (82)Rb PET myocardial perfusion imaging: a Danish multicenter study. Circ Cardiovasc Imag 2023;16:e015184.
[110] Fukushima K, Javadi MS, Higuchi T, Lautamäki R, Merrill J, Nekolla SG, et al. Prediction of short-term cardiovascular events using quantification of global myocardial flow reserve in patients referred for clinical 82Rb PET perfusion imaging. J Nucl Med 2011;52:726–32.
[111] Herzog BA, Husmann L, Valenta I, Gaemperli O, Siegrist PT, Tay FM, et al. Long-term prognostic value of 13N-ammonia myocardial perfusion positron emission tomography added value of coronary flow reserve. J Am Coll Cardiol 2009;54:150–6.
[112] Bom MJ, van Diemen PA, Driessen RS, Everaars H, Schumacher SP, Wijmenga JT, et al. Prognostic value of [15O]H2O positron emission tomography-derived global and regional myocardial perfusion. Eur Heart J Cardiovasc Imag 2020;21:777–86.
[113] van Diemen PA, Wijmenga JT, Driessen RS, Bom MJ, Schumacher SP, Stuijfzand WJ, et al. Defining the prognostic value of [15O]H2O positron emission tomography-derived myocardial ischaemic burden. Eur Heart J Cardiovasc Imag 2021;22:638–46.
[114] Siontis KC, Chareonthaitawee P. Prognostic value of positron emission tomography myocardial perfusion imaging beyond traditional cardiovascular risk factors: systematic review and meta-analysis. Int J Cardiol Heart Vasc 2015;6:54–9.
[115] de Winter RW, Jukema RA, van Diemen PA, Schumacher SP, Somsen YBO, van de Hoef TP, et al. Prognostic value of modified coronary flow capacity derived from [15O]H2O positron emission tomography perfusion imaging. Circul Cardio Imag 2023;16:e014845.
[116] Taqueti VR, Hachamovitch R, Murthy VL, Naya M, Foster CR, Hainer J, et al. Global coronary flow reserve is associated with adverse cardiovascular events independently of luminal angiographic severity and modifies the effect of early revascularization. Circulation 2015;131:19–27.
[117] Gould KL, Kitkungvan D, Johnson NP, Nguyen T, Kirkeeide R, Bui L, et al. Mortality prediction by quantitative PET perfusion expressed as coronary flow capacity with and without revascularization. J Am Coll Cardiol 2021;14:1020–34.
[118] Hachamovitch R, Hayes SW, Friedman JD, Cohen I, Berman DS. Comparison of the short-term survival benefit associated with revascularization compared with medical therapy in patients with No prior coronary artery disease undergoing stress myocardial perfusion single photon emission computed tomography. Circulation 2003;107:2900–7.
[119] Patel KK, Spertus JA, Chan PS, Sperry BW, Thompson RC, Al Badarin F, et al. Extent of myocardial ischemia on positron emission tomography and survival benefit with early revascularization. J Am Coll Cardiol 2019;74:1645–54.
[120] Lehtonen E, Kujala I, Tamminen J, Maaniitty T, Saraste A, Teuho J, et al. Incremental prognostic value of downstream positron emission tomography perfusion imaging after coronary computed tomography angiography: a study using machine learning. Europ Heart J Cardio Imag 2023;25:285–92.
[121] Driessen RS, Bom MJ, van Diemen PA, Schumacher SP, Leonora RM, Everaars H, et al. Incremental prognostic value of hybrid [15O]H2O positron emission tomography–computed tomography: combining myocardial blood flow, coronary stenosis severity, and high-risk plaque morphology. Europ Heart J Cardio Imag 2020;21:1105–13.
[122] Maaniitty T, Stenström I, Bax JJ, Uusitalo V, Ukkonen H, Kajander S, et al. Prognostic value of coronary CT angiography with selective PET perfusion imaging in coronary artery disease. JACC Cardiovasc Imag 2017;10:1361–70.
[123] Dobrolinska MM, Jukema RA, van Velzen SGM, van Diemen PA, Greuter MJW, Prakken NHJ, et al. The

prognostic value of visual and automatic coronary calcium scoring from low-dose computed tomography-[15O]-water positron emission tomography. Europ Heart J Cardio Imag 2024:jeae081.
[124] Johnson NP, Gould KL. Integrating noninvasive absolute flow, coronary flow reserve, and ischemic thresholds into a comprehensive map of physiological severity. JACC Cardiovasc Imag 2012;5:430–40.
[125] Collet C, Sonck J, Vandeloo B, Mizukami T, Roosens B, Lochy S, et al. Measurement of hyperemic pullback pressure gradients to characterize patterns of coronary atherosclerosis. J Am Coll Cardiol 2019;74:1772–84.
[126] Valenta I, Quercioli A, Schindler TH. Diagnostic value of PET-measured longitudinal flow gradient for the identification of coronary artery disease. J Am Coll Cardiol 2014;7:387–96.
[127] Gould KL, Nguyen T, Johnson NP. Integrating coronary physiology, longitudinal pressure, and perfusion gradients in CAD: measurements, meaning, and mortality. J Am Coll Cardiol 2019;74:1785–8.
[128] Bom MJ, Driessen RS, Raijmakers PG, Everaars H, Lammertsma AA, van Rossum AC, et al. Diagnostic value of longitudinal flow gradient for the presence of haemodynamically significant coronary artery disease. Europ Heart J Cardio Imag 2018;20:21–30.
[129] Hernandez-Pampaloni M, Keng FYJ, Kudo T, Sayre JS, Schelbert HR. Abnormal longitudinal, base-to-apex myocardial perfusion gradient by quantitative blood flow measurements in patients with coronary risk factors. Circulation 2001;104:527–32.
[130] Shiono Y, Kubo T, Honda K, Katayama Y, Aoki H, Satogami K, et al. Impact of functional focal versus diffuse coronary artery disease on bypass graft patency. Int J Cardiol 2016;222:16–21.
[131] Mizukami T, Sonck J, Sakai K, Ko B, Maeng M, Otake H, et al. Procedural outcomes after percutaneous coronary interventions in focal and diffuse coronary artery disease. J Am Heart Assoc 2022;11:e026960.
[132] Rimoldi O, Schäfers KP, Boellaard R, Turkheimer F, Stegger L, Law MP, et al. Quantification of subendocardial and subepicardial blood flow using 15O-labeled water and PET: experimental validation. J Nucl Med 2006;47:163–72.
[133] Gould KL, Nguyen T, Kirkeeide R, Roby Amanda E, Bui L, Kitkungvan D, et al. Subendocardial and transmural myocardial ischemia. J Am Coll Cardiol 2023;16:78–94.
[134] Sciagrà R, Milan E, Giubbini R, Kubik T, Di Dato R, Gallo L, et al. Sub-endocardial and sub-epicardial measurement of myocardial blood flow using 13NH3 PET in man. J Nucl Cardiol 2020;27:1665–74.
[135] Gould KL, Johnson Nils P. Coronary physiology beyond coronary flow reserve in microvascular angina. J Am Coll Cardiol 2018;72:2642–62.
[136] Di Carli MF, Brown JM. Probing the depths: subendocardial ischemia and clinical outcomes. JACC Cardiovasc Imag 2023;16:95–7.
[137] Rizvi A, Han D, Danad I, Ó Hartaigh B, Lee JH, Gransar H, et al. Diagnostic performance of hybrid cardiac imaging methods for assessment of obstructive coronary artery disease compared with stand-alone coronary computed tomography angiography: a meta-analysis. J Am Coll Cardiol 2018;11:589–99.
[138] Nissen L, Winther S, Westra J, Ejlersen JA, Isaksen C, Rossi A, et al. Diagnosing coronary artery disease after a positive coronary computed tomography angiography: the Dan-NICAD open label, parallel, head to head, randomized controlled diagnostic accuracy trial of cardiovascular magnetic resonance and myocardial perfusion scintigraphy. Eur Heart J Cardiovasc Imaging 2018;19:369–77.
[139] Meijboom WB, Meijs MFL, Schuijf JD, Cramer MJ, Mollet NR, van Mieghem CAG, et al. Diagnostic accuracy of 64-slice computed tomography coronary angiography: a prospective, multicenter, multivendor study. J Am Coll Cardiol 2008;52:2135–44.
[140] Mittal Tarun K, Hothi Sandeep S, Venugopal V, Taleyratne J, O'Brien D, Adnan K, et al. The use and efficacy of FFR-CT. J Am Coll Cardiol 2023;16:1056–65.
[141] Brodov Y, Gransar H, Dey D, Shalev A, Germano G, Friedman JD, et al. Combined quantitative assessment of myocardial perfusion and coronary artery calcium score by hybrid 82Rb PET/CT improves detection of coronary artery disease. J Nucl Med 2015;56:1345–50.
[142] Zampella E, Acampa W, Assante R, Nappi C, Gaudieri V, Mainolfi CG, et al. Combined evaluation of regional coronary artery calcium and myocardial perfusion by (82)Rb PET/CT in the identification of obstructive coronary artery disease. Eur J Nucl Med Mol Imag 2018;45:521–9.
[143] Pieszko K, Shanbhag A, Killekar A, Miller RJH, Lemley M, Otaki Y, et al. Deep learning of coronary calcium scores from PET/CT attenuation maps accurately predicts adverse cardiovascular events. J Am Coll Cardiol 2023;16:675–87.
[144] Einstein AJ, Johnson LL, Bokhari S, Son J, Thompson RC, Bateman TM, et al. Agreement of visual estimation of coronary artery calcium from low-dose CT attenuation correction scans in hybrid PET/CT and SPECT/CT with standard agatston score. J Am Coll Cardiol 2010;56:1914–21.
[145] Mylonas I, Kazmi M, Fuller L, deKemp RA, Yam Y, Chen L, et al. Measuring coronary artery calcification using positron emission tomography-computed tomography attenuation correction images. Europ Heart J Cardio Imag 2012;13:786–92.
[146] Pieszko K, Shanbhag AD, Lemley M, Hyun M, Van Kriekinge S, Otaki Y, et al. Reproducibility of quantitative coronary calcium scoring from PET/CT attenuation maps: comparison to ECG-gated CT scans. Eur J Nucl Med Mol Imag 2022;49:4122–32.
[147] Gulati M, Levy PD, Mukherjee D, Amsterdam E, Bhatt DL, Birtcher KK, et al. 2021 AHA/ACC/ASE/CHEST/SAEM/SCCT/SCMR guideline for the evaluation and diagnosis of chest pain: a report of the American college of cardiology/American heart association joint committee on clinical practice guidelines. Circulation 2021;144:e368–454.
[148] Maron DJ, Hochman JS, Reynolds HR, Bangalore S, O'Brien SM, Boden WE, et al. Initial invasive or conservative strategy for stable coronary disease. N Engl J Med 2020;382:1395–407.
[149] Chaitman BR, Alexander KP, Cyr DD, Berger JS, Reynolds HR, Bangalore S, et al. Myocardial infarction in the ISCHEMIA trial: impact of different definitions on incidence, prognosis, and treatment comparisons. Circulation 2021;143:790–804.
[150] Hochman JS, Anthopolos R, Reynolds HR, Bangalore S, Xu Y, O'Brien SM, et al. Survival after invasive or conservative management of stable coronary disease. Circulation 2023;147:8–19.
[151] Patel KK, Spertus JA, Chan PS, Sperry BW, Al Badarin F, Kennedy KF, et al. Myocardial blood flow reserve assessed by positron emission tomography myocardial perfusion imaging identifies patients with a survival benefit from early revascularization. Eur Heart J 2020;41:759–68.
[152] Rajkumar CA, Foley MJ, Ahmed-Jushuf F, Nowbar AN, Simader FA, Davies JR, et al. A placebo-controlled trial of percutaneous coronary intervention for stable angina. N Engl J Med 2023;389:2319–30.

[153] Patel KK, Spertus JA, Arnold SV, Chan PS, Kennedy KF, Jones PG, et al. Ischemia on PET MPI may identify patients with improvement in angina and health status post-revascularization. J Am Coll Cardiol 2019;74:1734–6.
[154] Bober RM, Milani RV, Oktay AA, Javed F, Polin NM, Morin DP. The impact of revascularization on myocardial blood flow as assessed by positron emission tomography. Eur J Nucl Med Mol Imag 2019;46:1226–39.
[155] Schumacher SP, Stuijfzand WJ, de Winter RW, van Diemen PA, Bom MJ, Everaars H, et al. Ischemic burden reduction and long-term clinical outcomes after chronic total occlusion percutaneous coronary intervention. JACC Cardiovasc Interv 2021;14:1407–18.
[156] de Winter RW, Jukema RA, van Diemen PA, Schumacher SP, Driessen RS, Stuijfzand WJ, et al. The impact of coronary revascularization on vessel-specific coronary flow capacity and long-term outcomes: a serial [15O]H2O positron emission tomography perfusion imaging study. Eur Heart J Cardiovasc Imag 2022;23:743–52.
[157] Schindler Thomas H, Fearon William F, Pelletier-Galarneau M, Ambrosio G, Sechtem U, Ruddy Terrence D, et al. Myocardial perfusion PET for the detection and reporting of coronary microvascular dysfunction. J Am Coll Cardiol 2023;16:536–48.
[158] Taqueti VR, Solomon SD, Shah AM, Desai AS, Groarke JD, Osborne MT, et al. Coronary microvascular dysfunction and future risk of heart failure with preserved ejection fraction. Eur Heart J 2018;39:840–9.
[159] Benz Dominik C, Kaufmann Philippe A, von Felten E, Benetos G, Rampidis G, Messerli M, et al. Prognostic value of quantitative metrics from positron emission tomography in ischemic heart failure. J Am Coll Cardiol 2021;14:454–64.
[160] Dorbala S, Vangala D, Bruyere Jr J, Quarta C, Kruger J, Padera R, et al. Coronary microvascular dysfunction is related to abnormalities in myocardial structure and function in cardiac amyloidosis. JACC Heart Fail 2014;2:358–67.
[161] Majmudar MD, Murthy VL, Shah RV, Kolli S, Mousavi N, Foster CR, et al. Quantification of coronary flow reserve in patients with ischaemic and non-ischaemic cardiomyopathy and its association with clinical outcomes. Eur Heart J Cardiovasc Imag 2015;16:900–9.
[162] Srivaratharajah K, Coutinho T, deKemp R, Liu P, Haddad H, Stadnick E, et al. Reduced myocardial flow in heart failure patients with preserved ejection fraction. Circ Heart Fail 2016;9.
[163] Sciagrà R, Calabretta R, Cipollini F, Passeri A, Castello A, Cecchi F, et al. Myocardial blood flow and left ventricular functional reserve in hypertrophic cardiomyopathy: a (13)NH(3) gated PET study. Eur J Nucl Med Mol Imag 2017;44:866–75.
[164] Arnold JR, Kanagala P, Budgeon CA, Jerosch-Herold M, Gulsin GS, Singh A, et al. Prevalence and prognostic significance of microvascular dysfunction in heart failure with preserved ejection fraction. J Am Coll Cardiol 2022;15:1001–11.
[165] Saraste A, Knuuti J, Bengel F. Phenotyping heart failure by nuclear imaging of myocardial perfusion, metabolism, and molecular targets. Europ Heart J Cardio Imag 2023;24:1318–28.
[166] Rush CJ, Berry C, Oldroyd KG, Rocchiccioli JP, Lindsay MM, Touyz RM, et al. Prevalence of coronary artery disease and coronary microvascular dysfunction in patients with heart failure with preserved ejection fraction. JAMA Cardiol 2021;6:1130–43.
[167] John JE, Claggett B, Skali H, Solomon SD, Cunningham JW, Matsushita K, et al. Coronary artery disease and heart failure with preserved ejection fraction: the ARIC study. J Am Heart Assoc 2022;11:e021660.
[168] van der Velde N, Huurman R, Yamasaki Y, Kardys I, Galema TW, Budde RPJ, et al. Frequency and significance of coronary artery disease and myocardial bridging in patients with hypertrophic cardiomyopathy. Am J Cardiol 2020;125:1404–12.
[169] Bravo PE, Pinheiro A, Higuchi T, Rischpler C, Merrill J, Santaularia-Tomas M, et al. PET/CT assessment of symptomatic individuals with obstructive and non-obstructive hypertrophic cardiomyopathy. J Nucl Med 2012;53:407–14.
[170] Thomas M, Sperry BW, Peri-Okonny P, Malik AO, McGhie AI, Saeed IM, et al. Relative prognostic significance of positron emission tomography myocardial perfusion imaging markers in cardiomyopathy. Circul Cardio Imag 2021;14:e012426.
[171] Chih S, Chong AY, Erthal F, deKemp RA, Davies RA, Stadnick E, et al. PET assessment of epicardial intimal disease and microvascular dysfunction in cardiac allograft vasculopathy. J Am Coll Cardiol 2018;71:1444–56.
[172] Mc Ardle BA, Davies RA, Chen L, Small GR, Ruddy TD, Dwivedi G, et al. Prognostic value of rubidium-82 positron emission tomography in patients after heart transplant. Circ Cardiovasc Imaging 2014;7:930–7.
[173] Feher A, Srivastava A, Quail MA, Boutagy NE, Khanna P, Wilson L, et al. Serial assessment of coronary flow reserve by rubidium-82 positron emission tomography predicts mortality in heart transplant recipients. J Am Coll Cardiol 2020;13:109–20.
[174] Kitkungvan D, Johnson NP, Kirkeeide R, Haynie M, Carter C, Patel MB, et al. Design and rationale of the randomized trial of comprehensive lifestyle modification, optimal pharmacological treatment and utilizing PET imaging for quantifying and managing stable coronary artery disease (the CENTURY study). Am Heart J 2021;237:135–46.